19700001064
70N103608

NASA TECHNICAL NOTE

NASA TN D-5524

NASA TN D-5524

EXPERIMENTAL INVESTIGATION OF ALUMINIDE-COATED Ta-10W FOR HEAT-SHIELD APPLICATIONS

by Gregory R. Wichorek and Bland A. Stein

Langley Research Center
Langley Station, Hampton, Va.

NATIONAL AERONAUTICS AND SPACE ADMINISTRATION • WASHINGTON, D. C. • NOVEMBER 1969

1. Report No. NASA TN D-5524	2. Government Accession No.	3. Recipient's Catalog No.
4. Title and Subtitle EXPERIMENTAL INVESTIGATION OF ALUMINIDE-COATED Ta-10W FOR HEAT-SHIELD APPLICATIONS		5. Report Date November 1969
		6. Performing Organization Code
7. Author(s) Gregory R. Wichorek and Bland A. Stein		8. Performing Organization Report No. L-6624
		10. Work Unit No. 129-03-20-01-23
9. Performing Organization Name and Address NASA Langley Research Center Hampton, Va. 23365		11. Contract or Grant No.
		13. Type of Report and Period Covered Technical Note
12. Sponsoring Agency Name and Address National Aeronautics and Space Administration Washington, D.C. 20546		14. Sponsoring Agency Code

15. Supplementary Notes

16. Abstract

An experimental study was undertaken to determine the applicability of tin-aluminum-molybdenum-coated Ta-10W for heat-shield usage. A relatively simple heat-shield design with a corrugated skin was utilized to evaluate the aluminide-coated tantalum-alloy composite. Separate flat heat-shield panels and several nested curved shields mounted on a conical model were tested in static air under cyclic heating conditions to 2600° F (1700 K). The corrugated heat shields were able to accommodate large temperature differences between the shield and the underlying structure with no loss of structural integrity. The time to coating failure on the heat shields was substantially less than that predicted from small-coupon data under static conditions. In view of the oxidation performance of the heat shields and the scatter in coupon data, methods to detect or recognize nonuniformities in the coating and the substrate are needed to predict coating life reliably.

The coating life on small specimens as determined for 0.1-hour exposures from 2300° F to 2900° F (1535 K to 1865 K) under static air conditions was reduced by a factor of approximately 4 under subsonic airflow conditions. Most significant was the catastrophic failure of the leading-edge specimens as a result of substrate ignition shortly after the first evidence of coating failure at temperatures of 2600° F (1700 K) and above. Metallurgical examinations and tensile data indicate that embrittlement of the aluminide-coated Ta-10W sheet may be a serious problem when thin-gage sheet is used at temperatures from 2300° F to 2900° F (1535 K to 1865 K).

17. Key Words Suggested by Author(s)	18. Distribution Statement
Heat shields Ta-10W Aluminide coating	Unclassified – Unlimited

19. Security Classif. (of this report)	20. Security Classif. (of this page)	21. No. of Pages	22. Price*
Unclassified	Unclassified	64	$3.00

*For sale by the Clearinghouse for Federal Scientific and Technical Information
Springfield, Virginia 22151

EXPERIMENTAL INVESTIGATION OF ALUMINIDE-COATED Ta-10W FOR HEAT-SHIELD APPLICATIONS

By Gregory R. Wichorek and Bland A. Stein
Langley Research Center

SUMMARY

An experimental study was undertaken to determine the applicability of tin-aluminum-molybdenum-coated Ta-10W for heat-shield usage. A relatively simple heat-shield design with a corrugated skin was utilized to evaluate the aluminide-coated tantalum-alloy composite. Separate flat heat-shield panels and several nested curved shields mounted on a conical model were tested in static air under cyclic heating conditions to 2600° F (1700 K). The corrugated heat shields were able to accommodate large temperature differences between the shield and the underlying structure with no loss of structural integrity. The time to coating failure on the heat shields was substantially less than that predicted from small-coupon data under static conditions. In view of the oxidation performance of the heat shields and the scatter in coupon data, methods to detect or recognize nonuniformities in the coating and the substrate are needed to predict coating life reliably.

The coating life on small specimens as determined for 0.1-hour exposures from 2300° F to 2900° F (1535 K to 1865 K) under static air conditions was reduced by a factor of approximately 4 under subsonic airflow conditions. Most significant was the catastrophic failure of the leading-edge specimens as a result of substrate ignition shortly after the first evidence of coating failure at temperatures of 2600° F (1700 K) and above. Metallurgical examinations and tensile data indicate that embrittlement of the aluminide-coated Ta-10W sheet may be a serious problem when thin-gage sheet is used at temperatures from 2300° F to 2900° F (1535 K to 1865 K).

INTRODUCTION

One possible application for coated refractory metals is as heat shields in forward fuselage and wing leading-edge regions of hypersonic airplanes. (See refs. 1 and 2.) A material being considered for this application is the tin-aluminum-molybdenum coating on tantalum alloy because of its promising oxidation resistance as exhibited on small coupons and its relative ease of application to large components. (See refs. 3 and 4.) Although certain low-pressure, high-temperature environments can degrade the coating, the poor low-pressure behavior of the coating is not considered detrimental for hypersonic airplane application where minimum operating ambient pressures on the order of 5 torr (0.67 kN/m^2) are expected.

No data are known to exist in the literature on the performance of full-size, thin-gage heat shields fabricated from tantalum alloys with protective coatings and particularly for several heat shields nested in a realistic arrangement for hypersonic vehicle applications. Therefore, an experimental study was undertaken to determine the applicability of the coated refractory-metal system for heat-shield usage under various conditions and environments. The structural integrity of corrugated heat shields subjected to high-temperature cycling in static air was investigated for individual shields and for several nested shields attached to a superalloy substructure. The effect of component size on the static oxidation performance of the coated refractory-metal system was determined from heat-shield and small-coupon tests with cyclic exposures to 2600° F (1700 K). Of equal interest was the effect of flowing air as compared with static air on the oxidation performance of the coated tantalum-alloy system for cyclic exposures in the temperature range of 2000° F to 2900° F (1365 K to 1865 K). In addition, the effects of the coating process and high-temperature exposure on the room-temperature properties of the tantalum-alloy substrate were investigated.

This experimental study was concerned initially with evaluating the coating of tin, 27 percent aluminum, and 5.5 percent molybdenum on Ta-10W. Because preliminary results showed this coating to have poor oxidation resistance in a high-temperature airstream, the composition was modified to tin, 27.5 percent aluminum, and 6.9 percent molybdenum to increase coating viscosity at elevated temperatures, which would hopefully improve the performance of the coating. Coating development and scale-up for large components was achieved by Sylvania Electric Products, Inc., under the sponsorship of the U.S. Air Force. Preliminary results from oxidation and mechanical-property specimens were reported in the Tenth and Thirteenth Refractory Composites Working Group reports. (See refs. 4 and 5.) The complete results of this experimental study are reported herein.

The units used for physical quantities in this paper are given both in the U.S. Customary Units and in the International System of Units (SI). (See ref. 6.) Conversion factors pertinent to the present investigation are presented in appendix A.

SPECIMENS AND COATINGS

All specimens were fabricated at the NASA Langley Research Center from annealed sheets of double-arc-melted 90 percent tantalum and 10 percent tungsten. (All compositions reported herein are nominal mass percentages.) Nominal sheet thicknesses were 0.008 inch (0.20 mm) and 0.025 inch (0.64 mm).

The tantalum-alloy specimens were covered with either a coating of tin, 27 percent aluminum, and 5.5 percent molybdenum (Sn-27Al-5.5Mo) or a coating of tin, 27.5 percent aluminum, and 6.9 percent molybdenum (Sn-27.5Al-6.9Mo), hereinafter referred to as 5.5Mo and 6.9Mo aluminide coatings, respectively. Both coatings were applied to the Ta-10W specimens by Sylvania Electric Products, Inc., by using a vacuum slurry dipping technique which is described in reference 7.

Mechanical-Property Specimens

Tensile specimens were 6 inches (150 mm) long and 5/8 inch (16 mm) wide with a 2-inch (51-mm) gage section length reduced to 0.312 inch (7.92 mm) in width. Specimens were sheared and machined from Ta-10W sheets, 0.008 inch (0.20 mm) and 0.025 inch (0.64 mm) thick. The 5.5Mo and 6.9Mo aluminide coatings were applied to the tensile specimens, except for control specimens.

Tensile-shear specimens were fabricated by overlapping two sheets 1/2 inch (13 mm) and making a single spotweld at the center of the overlapped area. Specimens were made by using resistance- and heliarc-spotwelding techniques. For the resistance-spotwelded specimens, the sheets were 1/2 inch (13 mm) wide and 3 inches (76 mm) long, and for the heliarc-spotwelded specimens, the sheets were 5/8 inch (16 mm) wide and $2\frac{1}{4}$ inches (57 mm) long. Tensile-shear specimens were made with sheet thickness combinations of 0.008-inch (0.20-mm) joined to 0.025-inch (0.64-mm) and 0.025-inch (0.64-mm) joined to 0.025-inch (0.64-mm) for both welding techniques to duplicate heat-shield joints.

Oxidation Specimens

Oxidation coupons were 3/4 inch by $1\frac{1}{2}$ inches (19 mm by 38 mm) with 0.125-inch (3.2-mm) radii at the corners. Coupons were fabricated from the 0.008-inch-thick (0.20-mm) Ta-10W sheet. Edges were rounded by machine tumbling, and the 5.5Mo and 6.9Mo aluminide coatings were applied to the coupons.

Leading-edge specimens 1/2-inch (13-mm) bend radius by $1\frac{1}{2}$ inches (38 mm) wide, were fabricated from the 0.008-inch-thick (0.20-mm) tantalum-alloy sheet. The leading edges were also coated with the 5.5Mo and 6.9Mo aluminide coatings.

Heat-Shield Specimens

The basic heat-shield design used in this investigation is shown in figure 1. The corrugated skin and plugs were fabricated from 0.008-inch-thick (0.20-mm) Ta-10W sheet. Each corrugation had a pitch and depth of 1.50 and 0.19 inches (38.1 and 4.8 mm), respectively, and the flats were 0.25 inch (6.4 mm) wide. Hat-section stiffeners and support clips were formed from the 0.025-inch-thick (0.64-mm) tantalum-alloy sheet. Flat and curved configurations of this design were fabricated for panel and model testing.

Forming procedures used to fabricate the tantalum-alloy shields were similar to those applicable to stainless-steel sheet. The Ta-10W hat-section stiffeners were stress relieved for 3 hours at 2150° F (1450 K), in vacuum, several times during the hammer forming of the sheet. All heat shields were vacuum annealed for approximately 1 hour at 2800° F (1810 K) prior to shipment to the coating vendor.

Flat heat shields.- Five flat heat-shield panels were studied in this investigation. Each heat-shield panel consisted of a coated tantalum-alloy heat shield approximately $9\frac{1}{2}$ inches by 18 inches (240 mm by 460 mm), a 1-inch-thick (25-mm) layer of Fiberfrax fibrous insulation, and a structural panel of truss-core sandwich. (See fig. 2.) The components of a flat heat-shield panel are shown in figure 3.

All heat shields were identical except for joining methods and coating composition. For one shield, rivets were used to join the hat-section flanges to the flats in the corrugated skin and the support clips to the hat sections. (See fig. 4.) The rivets were machined from 0.125-inch (3.2-mm) Ta-10W rod. A special rivet design which reduces faying surface areas was used to obtain good coating coverage at riveted joints; rivet design details are given in reference 8. For the other four heat shields, the shield components were joined by spotwelds. A typical spotwelded shield is shown in figure 2. A resistance-spotwelding technique was employed on two of the shields, and a heliarc-spotwelding technique was employed on the remaining two shields. The two resistance-spotwelded heat shields were coated with the 5.5Mo aluminide coating. The two heliarc-spotwelded shields and the riveted heat shield, which were fabricated later in the study, were coated with the 6.9Mo aluminide coating. Mass per unit wetted area of the flat heat shields before and after coating is reported in table I(a). The coating mass is approximately 22 percent of the original shield mass.

Plugs to cover the access holes in the heat shields after assembly were formed from 0.008-inch-thick (0.20-mm) Ta-10W sheet. (See fig. 5.) The plugs were coated with the same aluminide coatings as were applied to the heat shields.

The 1-inch-thick (25-mm) layer of fibrous insulation used between the heat shield and the truss-core structure has a density of 6 lbm/ft^3 (96 kg/m^3). This ceramic-fiber blanket is approximately 50.9 percent Al_2O_3 and 46.8 percent SiO_2. Four $1\frac{3}{4}$-inch-diameter (44-mm) holes were cut in the layer of insulation at the support-clip locations. (See fig. 3.) After the shield was attached to the truss-core structure, the insulation that had been removed to form the holes was shredded and replaced in the holes in the insulating layer through the shield access holes.

The René 41 truss-core structure, approximately 7/16 inch by $9\frac{1}{2}$ inches by 18 inches (11 mm by 240 mm by 460 mm), consisted of an 0.008-inch-thick (0.20-mm) corrugated sheet having 60° (1.05 rad) corrugations with 1/8-inch (3.2-mm) flats which were seam welded to 0.020-inch-thick (0.51-mm) face sheets. Four 0.29-inch-diameter (7.4-mm) holes were drilled through the panel at the quarter points. At these four locations, a 2-inch-diameter (51-mm) layer of alumina from 0.005 to 0.010 inch (0.13 to 0.25 mm) thick was flame sprayed on the outer face of the structure (fig. 3) to prevent high-temperature reactions between the aluminide coating and the René 41 structure. On the opposite face of the panel, inconel nuts were mounted at the holes with nut retainers spotwelded to the face sheet. (See fig. 2.) The retainers were formed from 0.008-inch-thick (0.20-mm) René 41 sheet.

The heat shields were fastened to the truss-core structure with inconel socket-head screws and washers. (See fig. 3.) The shanks of the screws and the washers were flame sprayed with alumina approximately 0.010 inch (0.25 mm) thick.

Curved heat shields.- Six curved heat shields were designed to conform to a curved surface typical of a vehicle fuselage section. When assembled, the shields covered one-third the lateral surface area of the frustum of a cone. (See fig. 6.) Two shield sizes were developed by dividing the frustum in half parallel to the base and each half into three equal parts. Shield nesting was achieved by orienting the expansion joint (fig. 1) along the longitudinal seams and by overlapping the forward shields approximately 1/2 inch (13 mm) over the aft shields. The corrugated configuration was such that the corrugations were essentially continuous from the forward shields to the aft shields. These design details can be seen more clearly in the photographs of the conical model in figure 7. The model consisted of the coated tantalum-alloy curved heat shields, a layer of fibrous insulation, and a support structure.

A typical curved Ta-10W heat shield before coating is shown in figure 8. The curved-shield components were similar to the flat-shield components and were joined by resistance spotwelds on all six curved heat shields. The support-clip lengths varied circumferentially from a maximum length of 0.93 inch (23.6 mm) on the two center shields to a minimum length of 0.71 inch (18.0 mm) on the outer edges of the four adjacent shields to provide more insulation along the line of maximum heating. The clips at the trailing end of each shield were longer than the clips at the leading end to provide a gap between the overlapping shields. These clip variations would be expected when application to a vehicle surface is considered. All the curved heat shields were coated with the 5.5Mo aluminide coating. Masses per unit wetted area of the curved heat shields before and after coating are reported in table I(b). The coating mass is over 20 percent of the original shield mass.

Fiberfrax insulation, 6 lbm/ft^3 (96 kg/m^3) density, was used between the shields and structure. The blanket insulation was cut to approximate shield size and the thickness roughly tailored to the clip lengths of the shields. All dimensions were slightly oversize so that the resilient insulation was compressed when it was installed to allow for some shrinkage at elevated temperatures and to eliminate gaps between pieces of insulation. Treatment of insulation at the shield supports was identical to that used on the flat panels.

The support structure was basically a frustum of 10° (0.17 rad) half-angle cone. The conical structure had an overall length of approximately $55\frac{1}{2}$ inches (1.4 meters) and base diameters of approximately $14\frac{1}{2}$ and $35\frac{1}{2}$ inches (0.4 and 0.9 m). Basically, the model structure had 0.060-inch-thick (1.5-mm) longitudinal corrugations. René 41 plate 1/4 inch (6.4 mm) or more in thickness was used for rings. In the areas of heat-shield attachments, flat plates were welded to the structural corrugations and tapped for 10-32 NF screws. A 1/16-inch-thick (1.6-mm) layer of Fiberfrax paper insulation was attached to the plates in the areas of clip contact for compatibility. Stainless-steel screws and washers were used to fasten the heat shields to the structure. Washers, flame sprayed with a layer of alumina approximately 0.010 inch (0.25 mm) thick, were used under the screw heads.

EQUIPMENT AND PROCEDURES

Mechanical-Property Tests

Tensile tests.- Room-temperature tensile stress-strain tests were performed in a 120 000-pound-capacity (534-kN) universal hydraulic testing machine at the Langley Research Center. Nominal strain rates of 0.005 per minute to yield and 0.050 per minute from yield to failure were controlled by continuously monitoring head motion. Strains were measured with optical strain gages attached to both sides of the specimen and were read while the strain rate was maintained.

High-temperature tensile tests were performed in a 10 000-pound-capacity (44-kN) screw-driven testing machine at the Langley Research Center at the same strain rates used for the room-temperature tests. High-temperature strain determinations were made by calibrating head motion against specimen strain at room temperature. Details of the procedure are presented in reference 8. Specimen temperatures were achieved by resistance heating. Temperatures were measured with an optical pyrometer at a wave length of 0.65 μm. A coating emittance of 0.7 was assumed. Tensile specimens were exposed to the test temperature for 6 minutes before loading. Elongation measurements were made by using finely scribed pencil lines at 1/4-inch (6.4-mm) intervals along the specimen.

Weld tensile-shear tests.- The weld tensile-shear tests were performed at room temperature in a 10 000-pound-capacity (44-kN) screw-driven testing machine at the Langley Research Center. A loading head motion of 0.020 in./min (0.51 mm/min) was maintained to failure.

Oxidation Tests

Static oxidation.- Coupon specimens were exposed to static oxidation in air at 760 torr (101 kN/m^2) in vertical tube furnaces. Coupons rested on high-purity alumina boats which were suspended in the furnaces on platinum wires. Specimens were subjected to continuous and cyclic exposures at temperatures from 1800° F to 2900° F (1255 K to 1865 K). Continuous-exposure tests were terminated for metallurgical examinations at selected time intervals from 1 to 230 hours.

For the cyclic-exposure tests, coupons were rapidly inserted and removed from the furnace with intervening exposures to slowly moving air. One of the following exposure times was selected for each coupon: 0.1 hour, 0.5 hour, or 1.0 hour. Cyclic tests were terminated either after coating failure or after 125 cycles. Visual evidence of tantalum oxide constituted coating failure.

Dynamic oxidation.- Leading-edge specimens were exposed to dynamic oxidation in a subsonic arc-heated airstream exhausting to atmospheric pressure from a 4-inch-diameter (100-mm) nozzle with a mass flow of 0.4 lbm/sec (0.2 kg/s) of air. The specimens were inserted into the hot airstream and then moved toward the nozzle until the desired test temperature was reached. Specimens were subjected to 0.1-hour cycles at temperatures from 2000° F to 2900° F (1365 K to 1865 K). Temperatures were measured with an optical pyrometer at a wavelength of 0.65 μm and a coating emittance assumed to be 0.7. Tests were generally terminated when coating failure was observed.

Metallurgical examinations.- The metallurgical examinations consisted of microscopic examinations, X-ray diffraction studies, and microhardness measurements of as-coated and tested specimens. A diffraction record was obtained by exposing the specimen to CuK_α radiation on a diffractometer. Microhardness measurements were obtained on a microhardness tester by using a Knoop indenter with a 0.1-kilogram (0.98-N) load. Microhardness and substrate thickness measurement procedures are detailed in reference 9.

Heat-Shield Tests

Flat heat shields.- Cyclic oxidation testing of the flat heat shields was accomplished in a radiant-heating apparatus. A diagram of the test setup is shown in figure 9. Quartz-infrared lamps were mounted in grooved, gold-plated reflectors, which were water cooled. To provide sufficient lamp cooling, air was directed along the length of the lamp envelopes by one of two air manifolds. The specimen was isolated from the airstream by three quartz plates, which rested on the specimen enclosure. No air leakage was detected at the joints of the butted quartz plates. The specimen enclosure, approximately 16 inches by $25\frac{1}{2}$ inches (400 mm by 650 mm), was formed by water-cooled, gold-plated reflectors. A guard ring of foamed-alumina brick was placed around the flat heat-shield panel. Figure 10 is a photograph of the radiant-heating apparatus with the movable heater assembly in the half-closed position prior to test. Three-phase electrical power was distributed to the lamps from an ignitron power supply. Power was controlled by a computer which continuously compared heat-shield temperature response with a programed temperature-time history.

The programed temperature-time profile for the coated flat heat shields was 15 minutes to test temperature, 18 minutes at test temperature, and 15 minutes from test temperature to room temperature. The flat heat shields were subjected to test temperatures of 2600° F and 2900° F (1700 K and 1865 K). Three heat-shield panels were cyclically exposed to the 2600° F (1700 K) profile while one panel was cyclically exposed to the 2900° F (1865 K) profile until general coating failure was observed. Coating-failure criteria will be described subsequently. The fifth heat-shield panel was exposed to both the 2600° F and 2900° F (1700 K and 1865 K) profiles to obtain temperature distributions.

Six spring-loaded thermocouple probes contacted the underside of the coated heat shield through 5/16-inch (7.9-mm) holes in the structure and insulation (fig. 11); 13 chromel-alumel thermocouples were spotwelded to the truss-core structure. Thermocouple probes were also used for temperature control on the cyclically tested panels. Thermocouple-probe details and calibration data are given in appendix B.

Curved heat shields.- Behavior of the assembled curved heat shields to cyclic exposure in static air was obtained in a conically shaped radiant heater. The heater was composed of 38 identical flat lamp banks which were arranged in four polygonal-shaped sections enclosing the entire conical model. (See fig. 12.) Only nine of these lamp banks were needed to heat the set of six heat shields which were mounted on the lower surface at the front end of the model. The quartz-infrared lamps were mounted in grooved, gold-plated reflectors, which were water cooled. Three-phase electrical power was distributed and controlled as previously mentioned. The thermocouple probes described in appendix B were used to measure and control heat-shield temperatures. The programed temperature-time profile for the curved heat shields was 15 minutes to 2600° F (1700 K), 6 minutes at 2600° F (1700 K), and 15 minutes to room temperature. The curved shields were exposed to two of these temperature-time cycles. Prior to each cycle, half the heat-shield plugs were installed at room temperature and the other half were heated during insertion to determine whether coating damage due to insertion or removal of plugs could be minimized. Heat was supplied by a hot-air gun producing a molten tin layer in the coating on the plug and access-hole edges. Damaged plugs were replaced with new plugs for the second heating cycle. Edges of access holes as well as the outer edges of the shield were visually inspected for coating damage before and after each cycle.

Coating-failure criteria.- Coating failures were detected by visual examination of the outer corrugated skin for either tantalum oxide or a blistering of the aluminide coating. Obviously, the appearance of tantalum oxide at the outer surface was indicative of coating failure. Detection of inner-surface coating failure by a blister in the aluminide coating on the outer surface is illustrated in figure 13. A coating blister on the outer shield surface is shown in figure 13(a); the corresponding inner shield surface, shown in figure 13(b), clearly shows the coating failure.

Coating failures were determined to be either problem area or general. Problem failures were considered premature failures linked to shield design, fabrication, or non-uniformities in coating chemistry. Areas considered possible problem areas were the faying surfaces at spotwelds and rivets, edges of access holes, and heat-shield plugs. General failure was considered to be an exhaustion or natural termination of the protective process. General coating failure was defined as visual evidence of tantalum oxide in shield areas generally considered nonproblem areas.

RESULTS AND DISCUSSION

Mechanical-Property Specimens

Tensile tests.- The effect of the aluminide coatings on the room-temperature tensile properties of the tantalum-alloy sheets is indicated in figure 14. Stress and modulus measurements of the tensile tests were based on original sheet thicknesses before coating application. On this basis, the 5.5Mo and 6.9Mo aluminide coatings had little effect on the strength of the Ta-10W substrates. This method of modulus determination and the formation of a hard tantalum-aluminide layer adjacent to the tantalum-alloy substrates (ref. 3) resulted in a noticeable increase in stiffness for the coated 0.008-inch-thick (0.20-mm) sheets. The most significant effect of the aluminide coatings on the tantalum-alloy sheets was the reduction of 50 and 30 percent, respectively, in the elongation of the 0.008-inch and 0.025-inch (0.20-mm and 0.64-mm) sheets.

The effect of temperature on the tensile properties of the 5.5Mo and 6.9Mo aluminide-coated sheet specimens is shown in figure 15. The dashed lines cover the temperature area where no data were taken, and for clarity of presentation, the mechanical-property curves are drawn only through the data points for the 5.5Mo aluminide-coated sheet of 0.025-inch (0.64-mm) thickness. In the range from 1700° F to 2900° F (1200 K to 1865 K), no unusual behavior is apparent in the tensile properties of the 5.5Mo aluminide-coated Ta-10W sheet. However, an elongation of only 2 percent at approximately 1700° F (1200 K) is significantly low. As shown in figure 15, the elevated-temperature tensile properties of the 6.9Mo aluminide-coated Ta-10W sheet are in general agreement with the values and trends indicated for the 5.5Mo aluminide-coated sheet.

The effect of time at elevated temperature on the tensile properties of the 0.008-inch-thick (0.20-mm) tantalum-alloy sheet coated with the 5.5Mo aluminide coating is indicated in figure 16. Specimens were exposed in air at 2600° F (1700 K) for periods up to 5 hours and tested both at 2600° F (1700 K) and at room temperature after exposure. Again, elongation is significantly reduced. The room-temperature elongation of approximately 9 percent before exposure is reduced to only 1 percent after 5 hours exposure to 2600° F (1700 K). This decrease in elongation indicates a severe embrittling effect.

Weld tensile-shear tests.- Metallurgical examinations of welds showed some resistance spotwelds to have cracks as indicated by the lower photomicrograph in figure 17(a). Establishment of a welding schedule to produce crack-free resistance spotwelds was not achieved. However, completely crack-free welds were achieved with heliarc-spotwelding techniques as indicated by the photomicrograph in figure 17(b). Results of the weld tensile-shear tests are given in table II. Specimens were tested in the as-welded condition and after heat treatments. Heat-treated specimens had approximately the same weld strengths as the as-welded specimens for comparable sheet thicknesses and failure mode. Two types of failure were experienced by the resistance-spotwelded specimens – shear failure through the weld and nugget failure in which the sheet tore in the heat-affected zone around the weld nugget. Average weld strengths for both types of resistance-spotweld failures are compared in figure 17(c) along with the average weld strengths obtained from the nugget-type failures of the heliarc spotwelds. The resistance and heliarc spotwelds had adequate weld strengths for heat-shield applications, but the resistance spotwelds were obviously not adequate for the requirement of crack-free welds.

Oxidation Specimens

Static oxidation.- The oxidation protection afforded Ta-10W by the aluminide coatings was determined from cyclic exposures of coupon specimens under static conditions in air. The effect of temperature and cyclic exposure on the coating life for 5.5Mo and 6.9Mo aluminide-coated Ta-10W specimens is presented in figures 18 and 19, respectively. No significant difference in static oxidation life was indicated between the aluminide coatings for the conditions and temperatures of the investigation. Shorter cyclic exposures resulted in significant decreases in coating life for the 5.5Mo and 6.9Mo aluminide coatings. Considerable scatter in the coating life of 6.9Mo aluminide-coated coupons at 1800° F and 2000° F (1255 K and 1365 K) was experienced. Scatter in this type of oxidation data is considered inherent in the cyclic testing of coated refractory-metal systems and indicates a need for specimen inspection techniques to reveal nonuniformities in the coating and the substrate.

Dynamic oxidation.- The results obtained for leading-edge specimens held at various locations in an arc-heated subsonic airstream to achieve specimen temperatures from 2000° F to 2900° F (1365 K to 1865 K) for 0.1-hour cyclic exposures are presented in table III and figure 20. No significant difference in coating life was apparent between the 5.5Mo and 6.9Mo aluminide coatings under dynamic oxidation conditions. However, a comparison of the data in figure 20 with the data in figures 18 and 19 indicates that coating life of both aluminide coatings determined for 0.1-hour exposures from 2300° F to 2900° F (1535 K to 1865 K) under static conditions was reduced by a factor of approximately 4 under subsonic airstream conditions. Another significant result of these flowing-air tests (table III) was the appearance of catastrophic failure, as a result of substrate ignition, of the 5.5Mo and 6.9Mo aluminide-coated specimens shortly after the first evidence of coating failure at temperatures of 2600° F (1700 K) and above. Complete consumption of the leading edges by oxidation after ignition in the subsonic airstream (fig. 21) was prevented by immediate removal of the specimens from the airstream.

Diffusion.- The variation in substrate thickness loss with exposure time for 5.5Mo aluminide-coated Ta-10W coupons after various continuous and cyclic exposures from 2000° F to 2900° F (1365 K to 1865 K) is shown in figure 22. Photomicrographs indicating substrate thickness loss with increased exposure time are shown in reference 4. Figure 22 is a plot of the substrate loss measurements and indicates an increase in rate of substrate thickness loss from 2000° F to 2300° F (1365 K to 1535 K) and approximately the same rate of substrate thickness loss from 2300° F to 2900° F (1535 K to 1865 K) for a given exposure time. A possible explanation for this behavior may be a depletion of aluminum in the aluminum-tin zone of the coating because of a more rapid increase in the rate of formation of the aluminum oxide zone at the specimen surface compared with that of the aluminide zone with increasing temperature from 2300° F to 2900° F (1535 K to 1865 K). Similar results are observed in reference 10 for aluminide-coated Ta-10W.

Metallurgical examinations showed a thickening, brittle aluminide layer with a corresponding decrease in substrate thickness after high-temperature exposure in air. Previously presented tensile data show elongation to be significantly reduced after 5 hours exposure at 2600° F (1700 K). The data indicate that diffusion is a possible source of embrittlement of the coated sheet. This embrittlement may be a serious problem when thin-gage, aluminide-coated Ta-10W sheet is used at temperatures from 2300° F to 2900° F (1535 K to 1865 K).

Flat Heat Shields

Cyclic oxidation data with temperature-time profiles to 2600° F and 2900° F (1700 K and 1865 K) were generated with four of the five flat heat shields. The other shield was exposed to both temperature profiles to obtain temperature distributions rather than cyclic oxidation data. Several observations and metallurgical examinations pertaining to coating reactions during the cyclic oxidation testing were made and are presented in appendix C.

Temperature distributions.- Temperature distributions through heat-shield panel 1 with a 5.5Mo aluminide-coated shield are shown in figure 23. Thermocouple locations are given in figure 23(a) for correlation with the temperature-time histories given in figures 23(b) and 23(c). The temperature difference between the center of the heat-shield skin and center of the superalloy truss-core structure at maximum temperature conditions was 1440° F (800 K) during the 2600° F (1700 K) test and 1630° F (905 K) during the 2900° F (1865 K) test. Examination of the heat-shield panel after testing revealed no damage to the corrugated skin, support clips, and truss-core structure. The test data show that the heat-shield design can accommodate large temperature differences between shield and underlying structure as well as permit the use of superalloy fasteners for structural attachment.

Problem-area failures.- The static oxidation test results for 5.5Mo and 6.9Mo aluminide-coated Ta-10W heat shields under cyclic exposures are presented in table IV. Times and locations of problem failures are indicated in table IV. For the 5.5Mo aluminide-coated shield, coating failures were detected along the access-hole edges after 4 cycles as shown in figure 24(a). Coating failure is evident in most cases by the cocked plugs caused by oxide growth and coating blisters. It should be noted in table IV that shield 2 had a set of plugs inserted and removed from the access holes prior to panel assembly. Apparently, the frictional, shear-type loadings imposed on the coated edges by an additional insertion and removal of the plugs could not be accommodated without coating damage. The data suggest that the coated shield has limited reusability where disassembly is required unless a change in design and/or in assembly and disassembly methods can reduce the frictional, shear-type loadings imposed on the access-hole edges.

The 6.9Mo aluminide-coated shields (shields 3 and 5) experienced problem failures at approximately the same time as shield 2. (See table IV.) The problem areas in these shields were at the weld faying surfaces for shield 3 (fig. 25(a)) and at the rivet heads for shield 5 (fig. 26). For these 6.9Mo aluminide-coated shields, failure was attributed, at least in part, to the increased viscosity of this coating over the 5.5Mo aluminide coating. An increase in coating viscosity could reduce the mobility of the Sn-Al phase and thereby decrease the self-healing characteristics and coating life. The transport rate of aluminum in the liquid Sn-Al phase is of importance in areas of welds and rivets where coating cracks may develop as a result of faying surfaces and stress concentrations. The possibilities of weld cracking and failure on the 5.5Mo aluminide-coated shield were greater than on the 6.9Mo aluminide-coated shield because of inferior resistance spotwelds, previously indicated in figure 17. Since no coating failures occurred at weld areas on the 5.5Mo aluminide-coated shield after 10 cycles and several coating failures were evident at weld areas on the 6.9Mo aluminide-coated shield after 4 cycles, the increased viscosity of the 6.9Mo aluminide coating was considered to be a factor in the early coating failures.

General coating failures.- By assuming the problem-area failures could be overcome by changes in design, fabrication, or coating processing, the aluminide coatings would be expected to provide oxidation protection until general coating failure occurred. The times of general coating failures for the aluminide-coated shields are given in table IV. Figures 24(b), 25(b), 26, and 27 show the appearance of these failures. In figure 28 aluminide-coating life on tantalum-alloy heat shields is compared with life estimated from small coupons. The 0.3-hour cyclic curves for coupons were obtained from straight-line interpolation of cycles to coating failure and then converted to time to failure in hours. Coating life was determined in this manner, since the performance of the coating is not only dependent on cumulative time at maximum temperature but also on the time accumulated during heating and cooling. The 5.5Mo and 6.9Mo aluminide-coated shields had general coating failures at approximately half the estimated failure time in the 2600° F (1700 K) tests. (See fig. 28.) The 6.9Mo aluminide-coated shield tested under 2900° F (1865 K) profile conditions had failures after 2 cycles or a time of 0.6 hour, which is approximately 15 percent of the coating failure time estimated from coupon data. The static oxidation results for the coated tantalum-alloy systems indicate that coating life is significantly lower on sizable complex parts than on small coupons. In view of the oxidation performance of the heat shields and the scatter in coupon data, methods to detect or recognize nonuniformities in the coating and the substrate are needed to predict coating life reliably.

Curved Heat Shields

The six curved shields were subjected to two 2600° F (1700 K) cycles, each with a time period of 0.1 hour at temperature. These cycles were preceded by an aborted cycle where, at shutdown, a peak temperature of 2100° F (1420 K) had been achieved. Maximum shield temperatures measured at the center of the shields and maintained during the 0.1-hour-cyclic hold periods are shown in figure 29. At the end of the hold period, a temperature difference of approximately 1730° F (960 K) was measured between the middle-aft shield and the structural surface. The curved shields were able to accommodate this temperature difference with no evidence of structural damage to corrugated skins and support clips.

Before and after each 2600° F (1700 K) cycle, heat-shield plugs were inserted and removed with or without heat as indicated in figure 29. Only two access-hole edges were damaged after the second 2600° F (1700 K) profile cycle. However, other coating damage and failures, as well as deformation of plug legs, were apparent on over 15 percent of the plugs after each cycle. An undetermined amount of coating was wiped away from the contacting plug and hole surfaces when plugs were inserted and removed with sufficient heat to form a molten tin layer; thus, plug insertion and removal appeared to be less detrimental to the coated surfaces at room temperature than with heat. A redesign of the heat-shield plug and access-hole feature is indicated to alleviate these problems.

The curved heat shields are shown in figure 30 after the aborted cycle where the maximum temperature was 2100° F (1420 K). The "icicles" hanging from the shields were formed from the liquid Sn-Al phase in the coating by the force of gravity in the static environment. During the next cycle or first cycle to 2600° F (1700 K), loss of coating by dripping was observed to be the greatest when shield temperatures were approximately 1200° F (920 K). Four oxidation failures on three shields were evident after the first cycle to 2600° F (1700 K). Two of the four oxidation failures and their locations can be seen in figure 31. These failures appeared, upon close examination of photographs, to be at locations where "icicles" had formed during the aborted cycle. This behavior in coatings with a liquid phase is an obvious detriment to the use of such coatings. The effect of flowing air, not present in these tests, might further aggravate the problem.

Although oxidation performance of the shields was poor, other equally important shield characteristics were noted for the coated refractory-metal system. On the basis of clearances after shield assembly, the design gaps were adequate to accommodate manufacturing tolerances. No apparent abrasive damage was found along shield surfaces and edges which may have come in contact with each other because of thermal expansion. Finally, fusion between interlocking shields and shield components was not in evidence after the 2600° F (1700 K) exposures even though the aluminide coating has a liquid phase.

CONCLUDING REMARKS

This experimental investigation was undertaken to determine the applicability of tin-aluminim-molybdenum-coated tantalum alloy for heat-shield usage. The following remarks are based on the results of the experimental study presented herein.

The corrugated heat-shield design can accommodate large temperature differences between shield and underlying structure with no loss of structural integrity. Early coating failures at the heat-shield plugs and access holes indicate that a change is needed in design and/or in assembly and disassembly methods to reduce the frictional, shear-type loadings on the coating. No apparent coating damage was found along overlapped surfaces and edges on the nested curved shields after two cyclic exposures to 2600° F (1700 K). Fusion between interlocking shields and shield components was not in evidence even though the aluminide coating has a liquid phase.

Under static conditions, the time to coating failure on the heat shields was substantially less than that predicted from small-coupon data. In view of the oxidation performance of the heat shields and the scatter in the coupon data, methods to detect or recognize nonuniformities in the coating and the substrate are needed to predict coating life reliably.

Coating life of both aluminide coatings on small specimens as determined for 0.1-hour exposures from 2300° F to 2900° F (1535 K to 1865 K) under static conditions was reduced by a factor of approximately 4 under subsonic airstream conditions. Most significant was the catastrophic failure of the leading-edge specimens as a result of substrate ignition shortly after the first evidence of coating failure at temperatures of 2600° F (1700 K) and above.

No significant difference in static oxidation life was indicated between the Sn-27Al-5.5Mo and Sn-27.5Al-6.9Mo coatings on coupons from 2000° F to 2900° F (1365 K to 1865 K) under the cyclic conditions of the investigation. Shorter cyclic exposures resulted in significant decreases in the coating life of both aluminide coatings.

Embrittlement of the aluminide-coated tantalum-alloy substrate may be a serious problem when thin-gage sheet is used at temperatures from 2300° F to 2900° F (1535 K to 1865 K). A critical example was a reduction in room-temperature elongation to only 1 percent after 5 hours exposure to 2600° F (1700 K).

Langley Research Center,
National Aeronautics and Space Administration,
Langley Station, Hampton, Va., August 26, 1969.

APPENDIX A

CONVERSION OF U.S. CUSTOMARY UNITS TO SI UNITS

Conversion factors (ref. 6) for the units used herein are given in the following table:

Physical quantity	U.S. Customary Unit	Conversion factor (*)	SI Unit (**)
Length	in.	2.54×10^{-2}	meters (m)
Mass	lbm	4.536×10^{-1}	kilograms (kg)
Force	lbf	4.448	newtons (N)
Stress or modulus . .	psi = lbf/in^2	6.895×10^{3}	newtons/$meter^2$ (N/m^2)
	ksi = kips/in^2	6.895×10^{6}	newtons/$meter^2$ (N/m^2)
Pressure	torr	1.333×10^{2}	newtons/$meter^2$ (N/m^2)
Mass per unit wetted area	lbm/ft^2	4.883	kilograms/$meter^2$ (kg/m^2)
Density	lbm/ft^3	1.602×10	kilograms/$meter^3$ (kg/m^3)
Temperature	^{o}F	$\frac{5}{9}(F + 460)$	kelvins (K)
Degrees (angle) . . .	^{o}	1.745×10^{-2}	radians (rad)

*Multiply value given in U.S. Customary Unit by conversion factor to obtain equivalent value in SI unit.

**Prefixes to indicate multiple of units are as follows:

Prefix	Multiple
micro (μ)	10^{-6}
milli (m)	10^{-3}
hecto (h)	10^{2}
kilo (k)	10^{3}
mega (M)	10^{6}
giga (G)	10^{9}

APPENDIX B

THERMOCOUPLE-PROBE DETAILS AND CALIBRATION DATA

Spring-loaded thermocouple probes were used to measure and control the temperature of the coated tantalum-alloy heat shields. The thermocouple probes were basically the same as the thermocouple probes reported in reference 8 except for changes in the sensing element and support components. The probe sensing element was a 3/16-inch (4.8-mm) square of 0.005-inch-thick (0.13-mm) rhodium foil to which No. 30 gage platinum—platinum-10 percent rhodium wires were spotwelded. A thin layer of molybdenum disilicide was sintered on the outer surface of the foil. The molybdenum disilicide was compatible with the aluminide coatings under the test temperatures and times, whereas the rhodium foil was not compatible. Probe calibration tests were performed to establish probe temperature, time lag, and repeatability of response compared with the contacted surface response. Calibration specimens were titanium-alloy plates, 0.060 by 6 by 6 inches (1.50 by 150 by 150 mm), backed with a 1-inch-thick (25-mm) layer of Fiberfrax insulation. A new plate was used for each calibration run because of oxidation. For use as a "standard," a platinum—platinum-10 percent rhodium thermocouple was spotwelded to the titanium-alloy plate 3/8 inch (9.5 mm) from the probe junction. Results of thermocouple calibration tests to determine temperature response of thermocouple probe compared with the spotwelded thermocouple are presented in figure 32. The temperature difference between probe and "standard" thermocouple was greater during heating than cooling, as shown in figure 32(b), because of variations in heat losses along the probe. All probe temperature measurements were adjusted in accordance with the average temperature response curves in figure 32(b).

APPENDIX C

OBSERVATIONS AND METALLURGICAL EXAMINATIONS OF COATED HEAT SHIELDS

The following observations and metallurgical examinations were made during the cyclic oxidation testing of the Sn-27Al-5.5Mo and Sn-27.5Al-6.9Mo coated heat shields. Some coating failures similar in appearance to the one described in this appendix occurred on coupon and leading-edge specimens.

Noticeable volatilization of the Sn-27Al-5.5Mo and Sn-27.5Al-6.9Mo coatings occurred during the first heating cycle on each heat shield as evidenced by a powdery deposit on the reflectors and quartz plates of the test enclosure. (See figs. 9 and 10.) The amount of deposit on succeeding cycles was negligible until coating failures occurred. A considerable increase in the amount of volatilization occurred from 2600° F to 2900° F (1700 K to 1865 K). Volatilization of the Sn-27.5Al-6.9Mo coating was so great during the first 2900° F (1865 K) cycle that a powdery deposit collected on the control thermocouple probe and apparently penetrated to and reacted with the platinum-rhodium sensing element. This reaction resulted in the termination of the test cycle after 11 minutes at 2900° F (1865 K). The control probe was replaced for the second heating cycle. Since volatilization of the coating while at test temperature was considerably reduced on the second cycle (this volatilization corresponded to coating behavior at 2600° F (1700 K)), the shield was held an additional 7 minutes at temperature for possible correlation with other cyclic data.

This heat-shield panel is shown in figure 27 after 3 cycles to 2900° F (1865 K). The dark area shown in figure 27(a) is yellow and black and, under close examination, has a fused appearance. In a few places along the edge of the hole, black crystals could be seen. No attempt was made to determine the constituents in this area. However, similar black crystals which had formed at a failure site on a Sn-27.5Al-6.9Mo heat shield tested at 2600° F (1700 K) were identified as SnO_2 (cassiterite) by using X-ray diffraction techniques. Disassembly of this heat-shield panel after coating failure revealed a white, powdery deposit on the inner surface of the corrugated shield. (See fig. 27(b).) The deposit covered the area under the hat sections to the flats in the corrugated skin just beyond the access holes. (See fig. 27(c).) This white powder was identified as αAl_2O_3 (corundum) by using X-ray diffraction techniques.

REFERENCES

1. Heldenfels, R. R.: Structural Prospects for Hypersonic Air Vehicles. ICAS Paper No. 66-31, 5th Congress Int. Council Aeron. Sci., Sept. 12-16, 1966.

2. Stein, Bland A.; Illg, Walter; and Buckley, John D.: Structural Materials for Hypersonic Aircraft. Conference on Hypersonic Aircraft Technology. NASA SP-148, 1967, pp. 485-499.

3. Lawthers, Dean D.; and Sama, L.: High Temperature Oxidation Resistant Coatings for Tantalum Base Alloys. ASD Tech. Rep. 61-233 (Contract AF33(616)-7462), U.S. Air Force, 1961.

4. Wichorek, Gregory R.; and Stein, Bland A.: Preliminary Results of a Study of Coated Ta-10W Sheet for Heat-Shield Applications. Summary of the Tenth Refractory Composites Working Group Meeting, AFML-TR-65-207, U.S. Air Force, Aug. 1965, pp. 203-215. (Available from DDC as AD472867.)

5. Stein, Bland A.; and Wichorek, Gregory R.: Results of Current Studies on Coated Tantalum Alloy Sheet at NASA Langley Research Center. Summary of the Thirteenth Refractory Composites Working Group Meeting, AFML-TR-68-84, U.S. Air Force, May 1968, pp. 261-280. (Available from DDC as AD838781.)

6. Comm. on Metric Pract.: ASTM Metric Practice Guide. NBS Handbook 102, U.S. Dep. Com., Mar. 10, 1967.

7. Sama, L.; and Reznik, B.: Development of Production Methods for High-Temperature Coating of Tantalum Parts. AFML-TR-66-217, U.S. Air Force, Aug. 1966. (Available from DDC as AD488447.)

8. Wichorek, Gregory R.; and Stein, Bland A.: Experimental Investigation of Insulating Refractory-Metal Heat-Shield Panels. NASA TN D-1861, 1964.

9. Stein, Bland A.; and Lisagor, W. Barry: Diffusion Studies of Several Oxidation Resistant Coatings on Mo-0.5Ti Molybdenum Alloy at 2,500° F. NASA TN D-2039, 1964.

10. Sama, L.: High-Temperature Oxidation-Resistant Coatings for Tantalum Base Alloys. ASD-TDR-63-160, U.S. Air Force, Feb. 1963.

TABLE I.- HEAT-SHIELD MASS PER UNIT WETTED AREA BEFORE AND AFTER ALUMINIDE-COATING APPLICATIONS

(a) Flat configurations

Heat shield	Mass/unit wetted area			
	Before coating		After coating	
	lbm/ft^2	kg/m^2	lbm/ft^2	kg/m^2
Sn-27Al-5.5Mo				
1	1.44	7.03	1.76	8.59
2	1.44	7.03	1.74	8.50
Sn-27.5Al-6.9Mo				
3	1.43	6.98	1.74	8.50
4	1.44	7.03	1.76	8.59
5	1.43	6.98	1.73	8.45

(b) Curved configurations

[Sn-27Al-5.5Mo coated]

Heat shield	Mass/unit wetted area			
	Before coating		After coating	
	lbm/ft^2	kg/m^2	lbm/ft^2	kg/m^2
1	1.45	7.08	1.77	8.64
2	1.46	7.13	1.77	8.64
3	1.46	7.13	1.77	8.64
4	1.48	7.23	1.79	8.74
5	1.48	7.23	1.79	8.74
6	1.48	7.23	1.77	8.64

TABLE II.- RESULTS OF WELD TENSILE-SHEAR TESTS ON SINGLE-SPOTWELDED Ta-10W SHEET SPECIMENS

Welding technique	Tensile-shear specimen			Failure load (a)		Type of failure
	Sheet thickness		Heat treatment			
	inch	mm		lbf	N	
Resistance spotwelding	0.008 joined to 0.025	0.20 joined to 0.64	----------------	164 165 181	729 734 805	Sheared through weld but had started pulling nugget
			----------------	205 210 212	912 934 943	Pulled nugget
			3 hours at 2150° F (1450 K)	198 215	881 956	Pulled nugget
			1 hour at 2800° F (1810 K)	220 226	979 1005	Pulled nugget
	0.025 joined to 0.025	0.64 joined to 0.64	----------------	505 521 522	2246 2317 2322	Sheared through weld
			3 hours at 2150° F (1450 K)	522 538	2322 2393	Sheared through weld
			1 hour at 2800° F (1810 K)	535 535	2380 2380	Sheared through weld
Heliarc spotwelding	0.008 joined to 0.025	0.20 joined to 0.64	----------------	227 [b]213	1010 [b]947	Pulled nugget
			1 hour at 2800° F (1810 K)	215	956	Pulled nugget
	0.025 joined to 0.025	0.64 joined to 0.64	----------------	711 [b]703	3163 [b]3127	Pulled nugget
			1 hour at 2800° F (1810 K)	725	3225	Pulled nugget

[a]Loading head motion: 0.020 in./min (0.51 mm/min) except where noted.
[b]Loading head motion: 0.005 in./min (0.13 mm/min).

TABLE III.- RESULTS OF OXIDATION TESTS ON ALUMINIDE-COATED Ta-10W LEADING-EDGE SPECIMENS IN AN ARC-HEATED, SUBSONIC AIR JET UNDER 0.1-HOUR CYCLIC CONDITIONS

Test temperature		Cumulative time to failure, hours	Cumulative time to ignition, hours
^{o}F	K		
Sn-27Al-5.5Mo			
2000	1365	>2.00	
2300	1535	1.10	
		>1.00	
2600	1700	0.40	
		.50	0.58
2900	1865	0.01	0.02
Sn-27.5Al-6.9Mo			
2000	1365	>2.00	
2300	1535	1.30	
2600	1700	0.62	
		>1.00	
2750	1785	0.55	0.56
2900	1865	0.02	0.03
		.30	.35

TABLE IV.- RESULTS OF STATIC OXIDATION TESTS ON ALUMINIDE-COATED Ta-10W HEAT SHIELDS UNDER CYCLIC EXPOSURE

Flat heat shield	Joining method	Cyclic temperature profile		Cumulative failure time				Problem area
				Problem		General		
		$^{\circ}F$	K	Cycles	Hours	Cycles	Hours	
Sn-27Al-5.5Mo								
2	Resistance spotwelds	2600	1700	4	1.2	9	2.7	[a]Access-hole edges
Sn-27.5Al-6.9Mo								
3	Heliarc spotwelds	2600	1700	4	1.2	11	3.3	Weld faying surfaces
5	Rivets	2600	1700	5	1.5	12	3.6	Rivet-head areas
4	Heliarc spotwelds	2900	1865	---	---	2	.6	------------------

[a]A set of plugs had been inserted and removed from holes before shield was assembled for test.

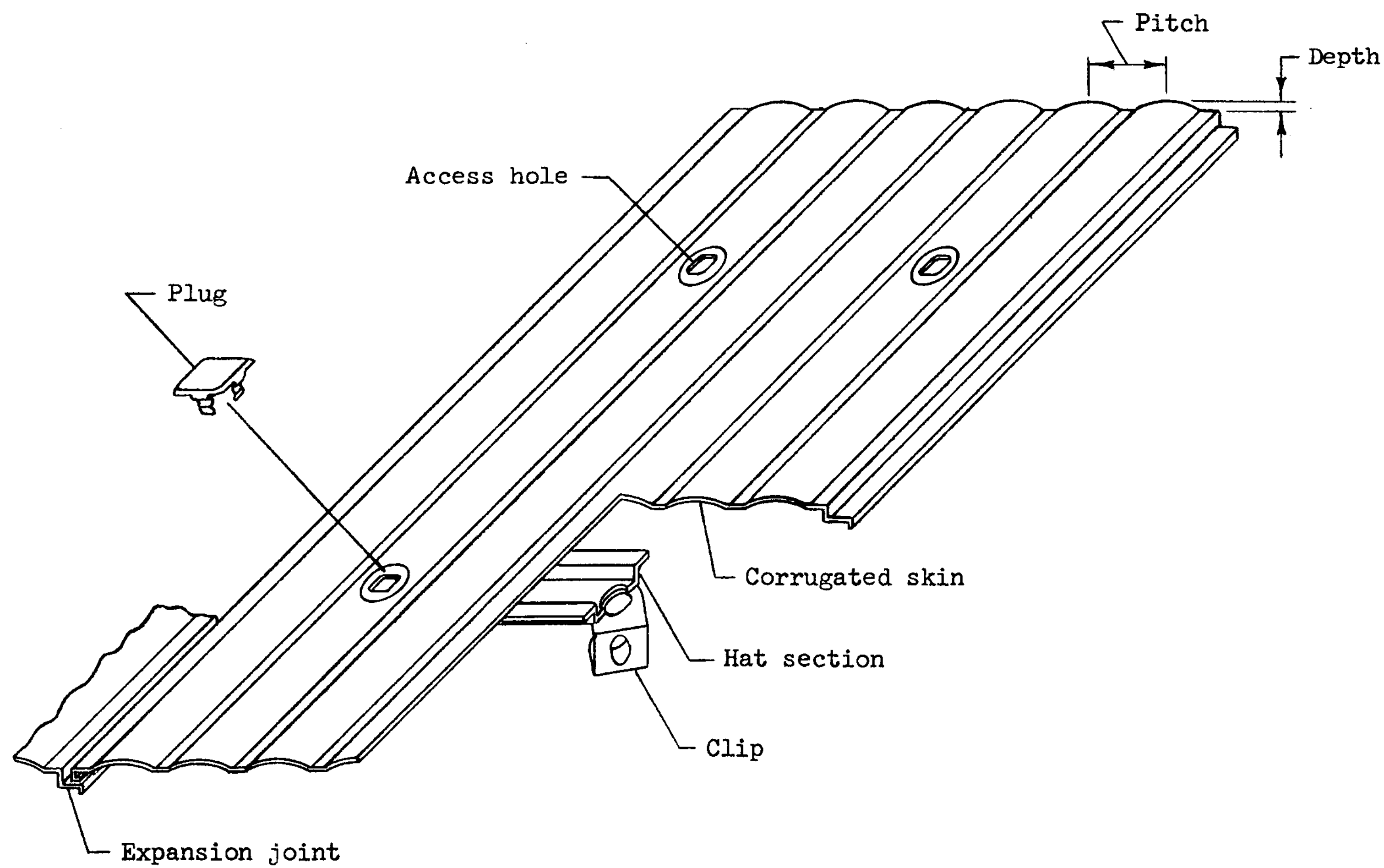

Figure 1.- Heat-shield design selected for flat- and curved-shield configurations fabricated from tantalum-alloy sheet.

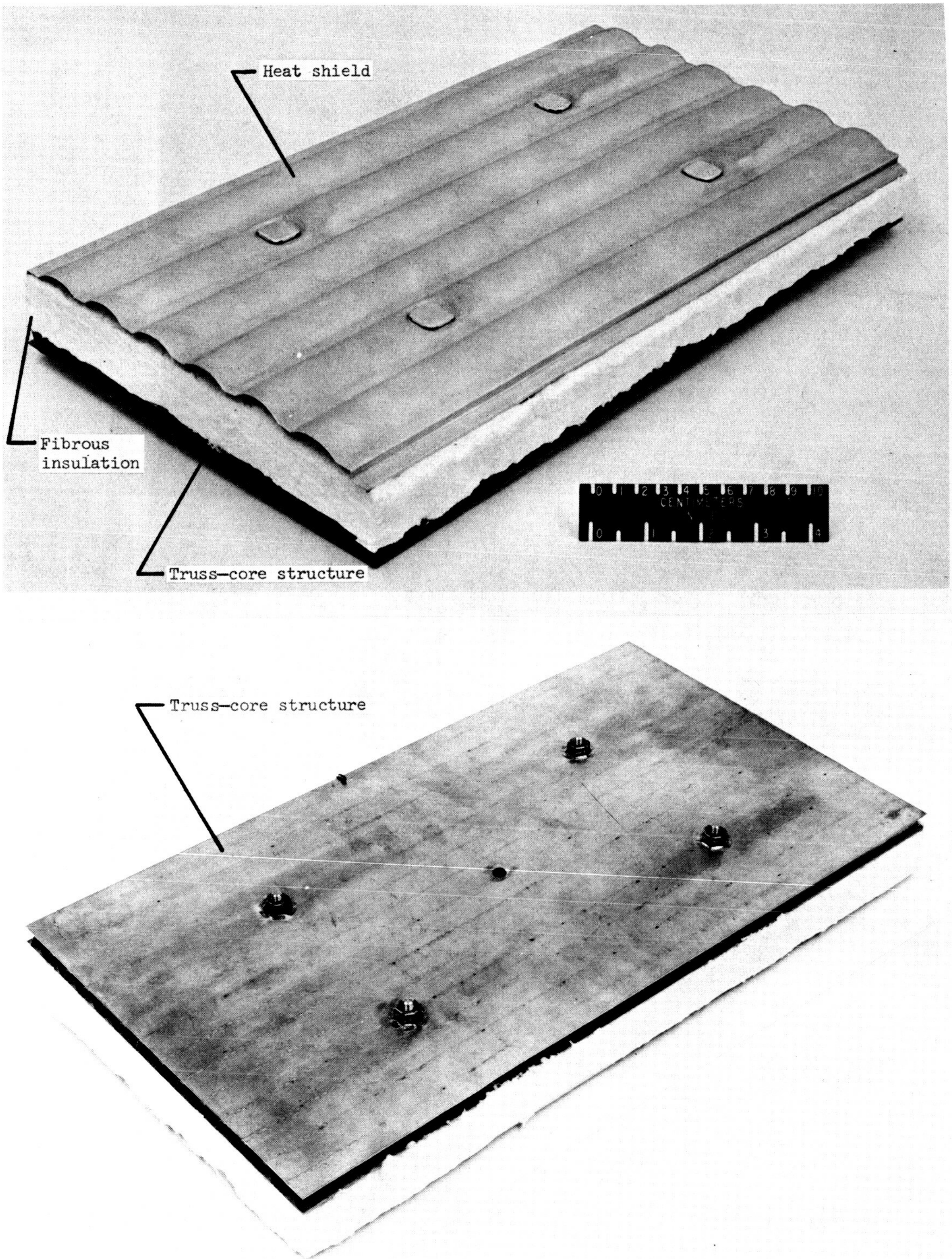

Figure 2.- Typical flat heat-shield panel with spotwelded joints after assembly.

L-69-5086

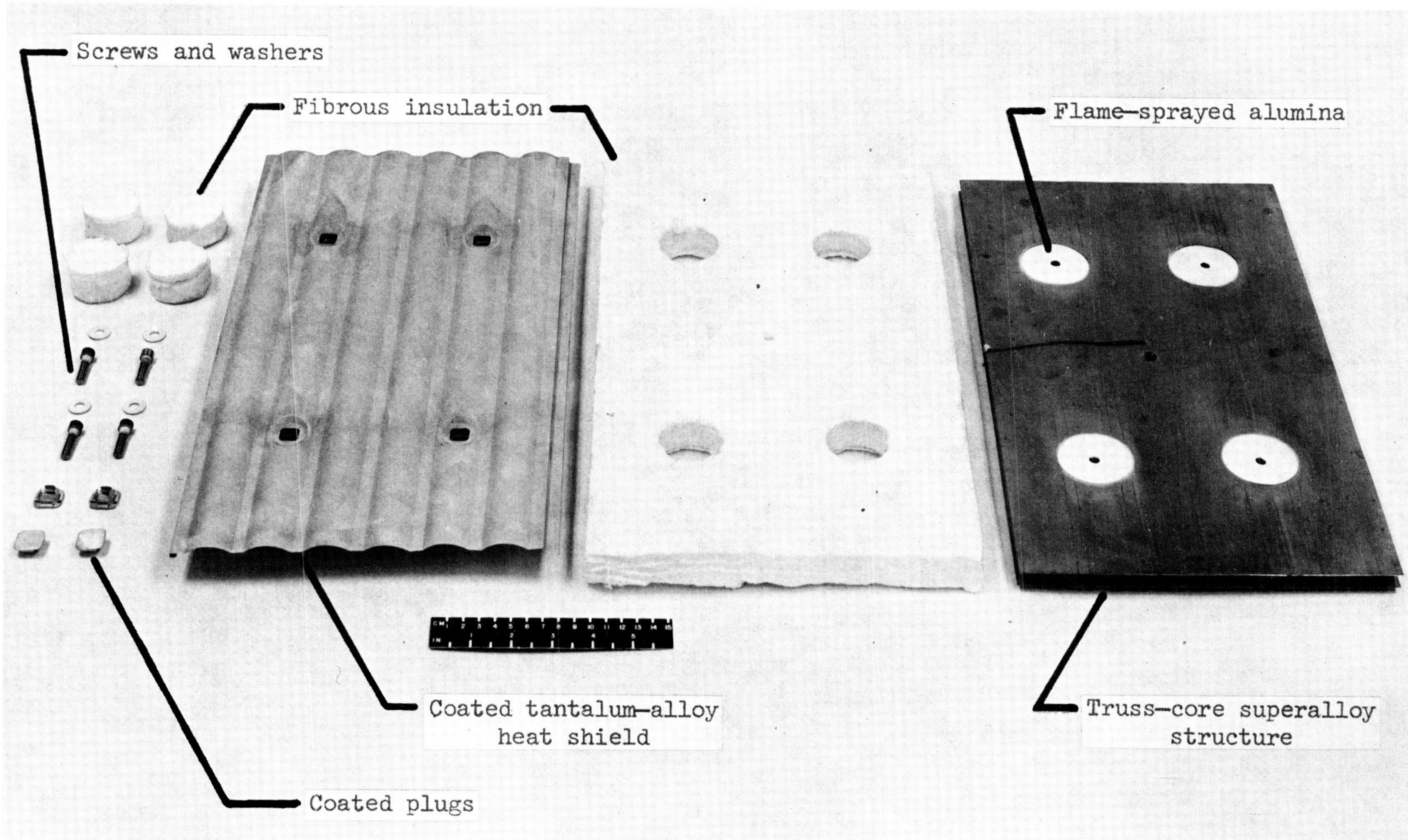

Figure 3.- Components of a typical flat heat-shield specimen.

L-68-2440.1

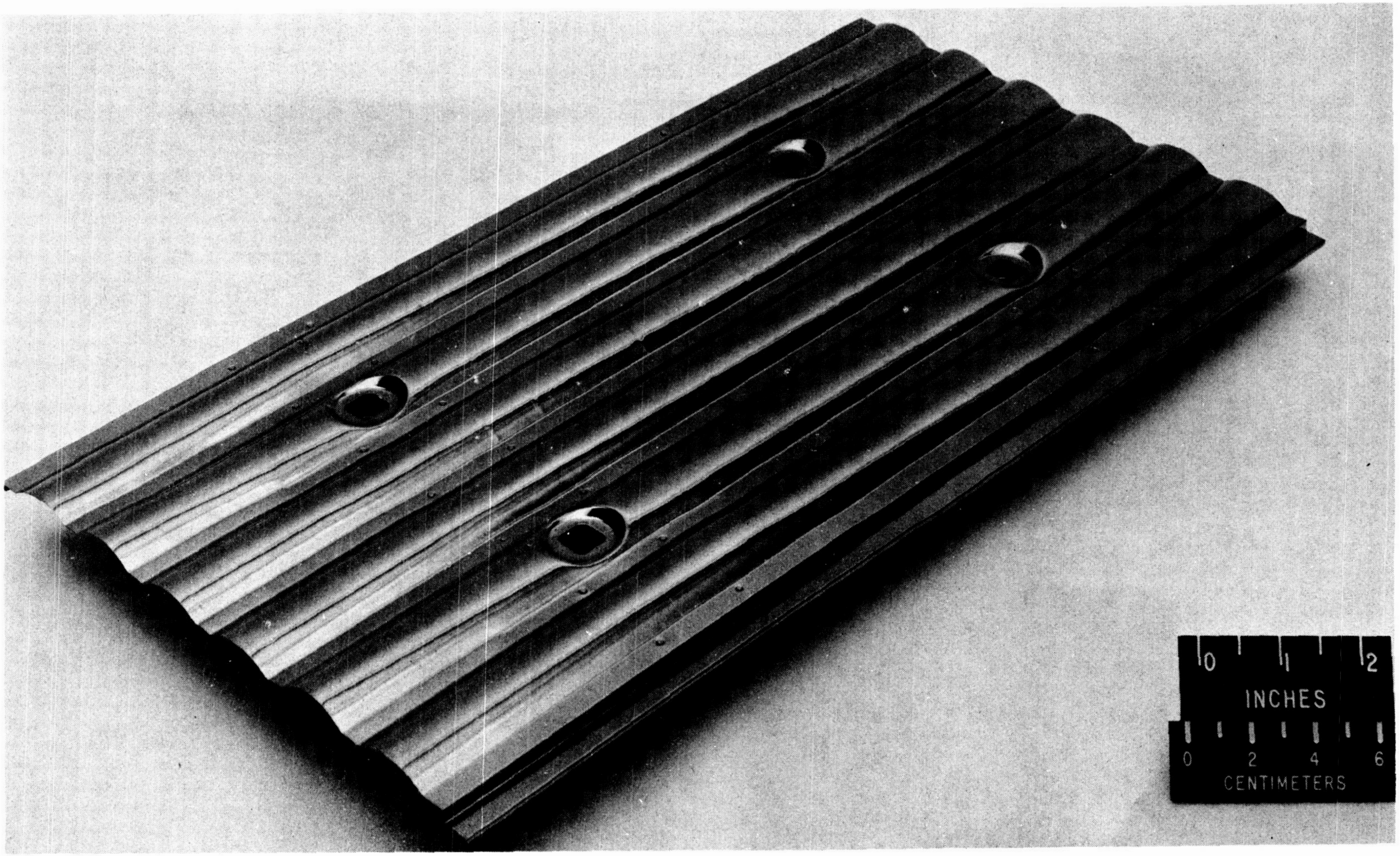

(a) Outer surface.

L-65-7069

Figure 4.- Ta-10W heat shield with riveted joints before coating.

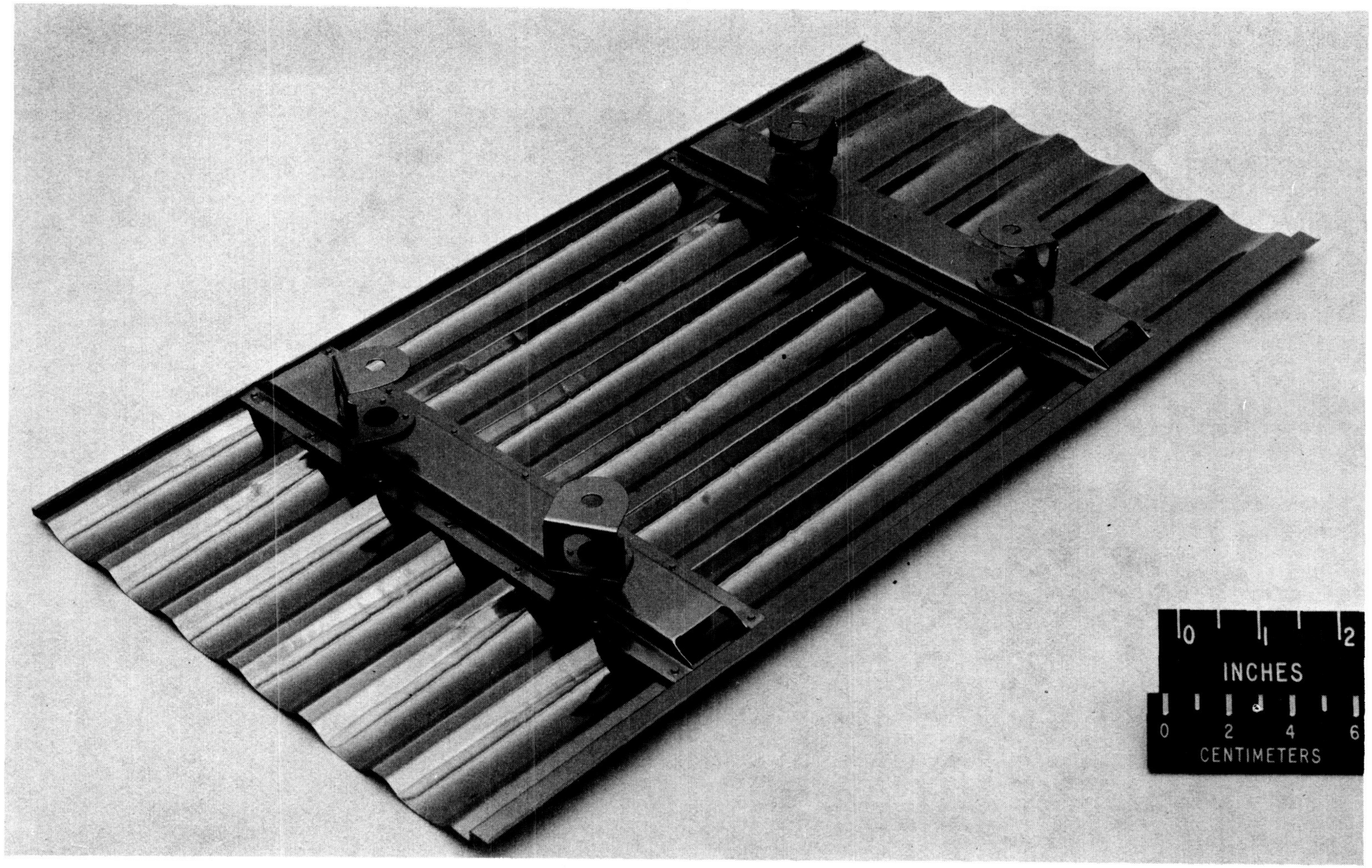

(b) Inner surface.

L-65-7074

Figure 4.- Continued.

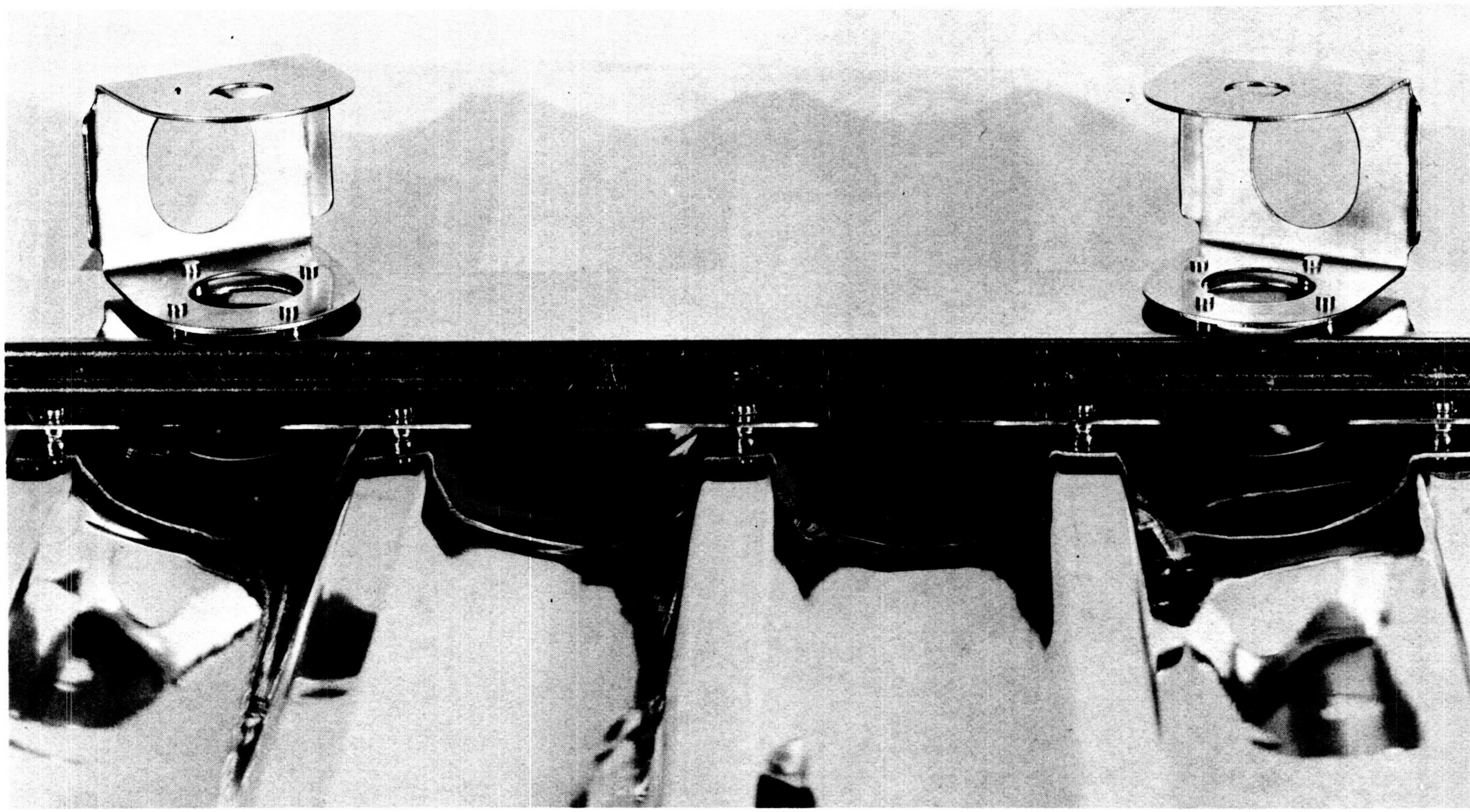

(c) Closeup showing riveted joints. L-65-7072

Figure 4.- Concluded.

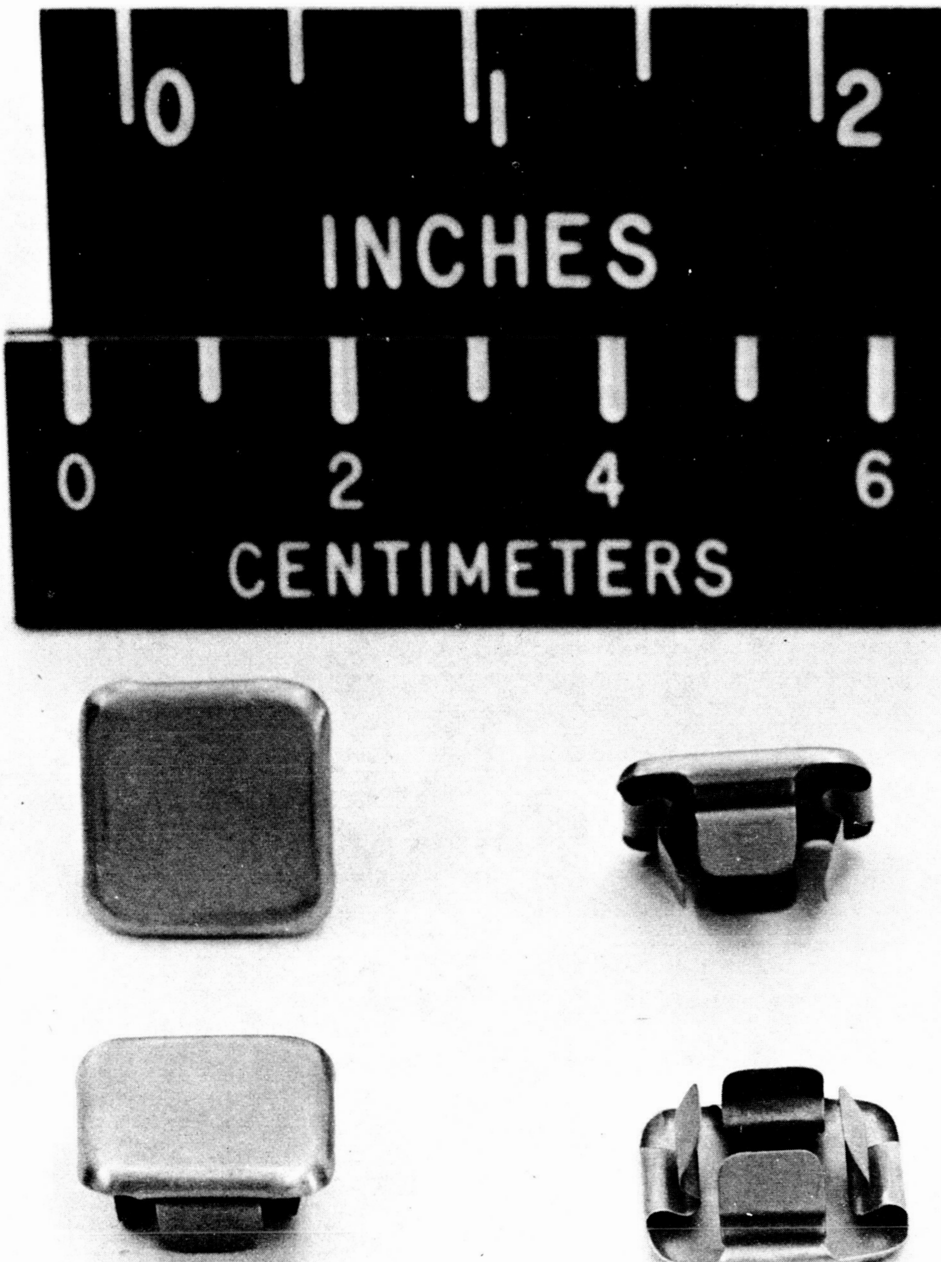

Figure 5.- Heat-shield plugs as-fabricated from 0.008-inch-thick (0.20-mm) Ta-10W sheet. L-65-835

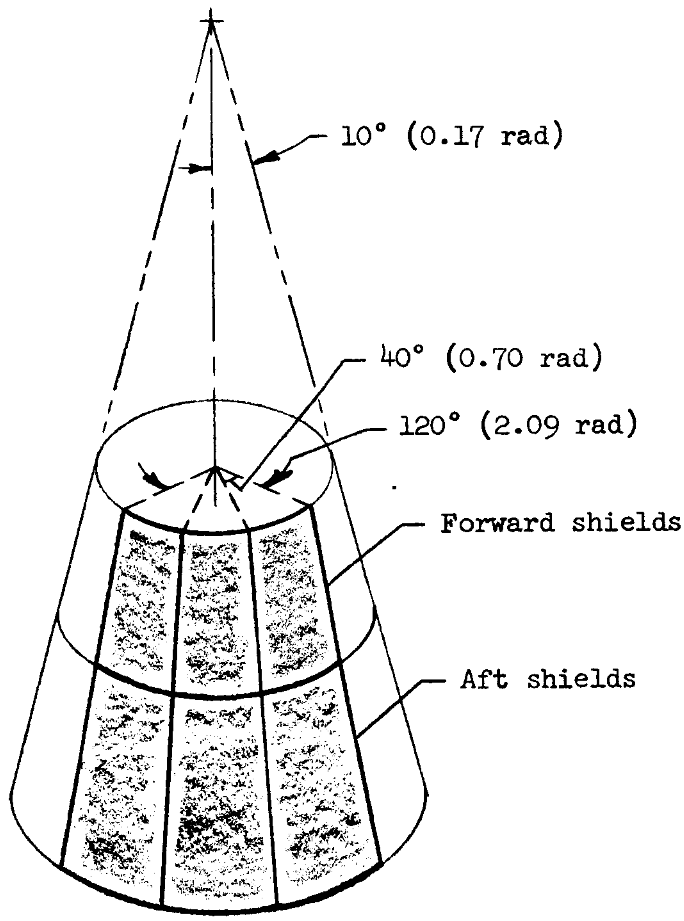

Figure 6.- Design configuration for curved heat shields.

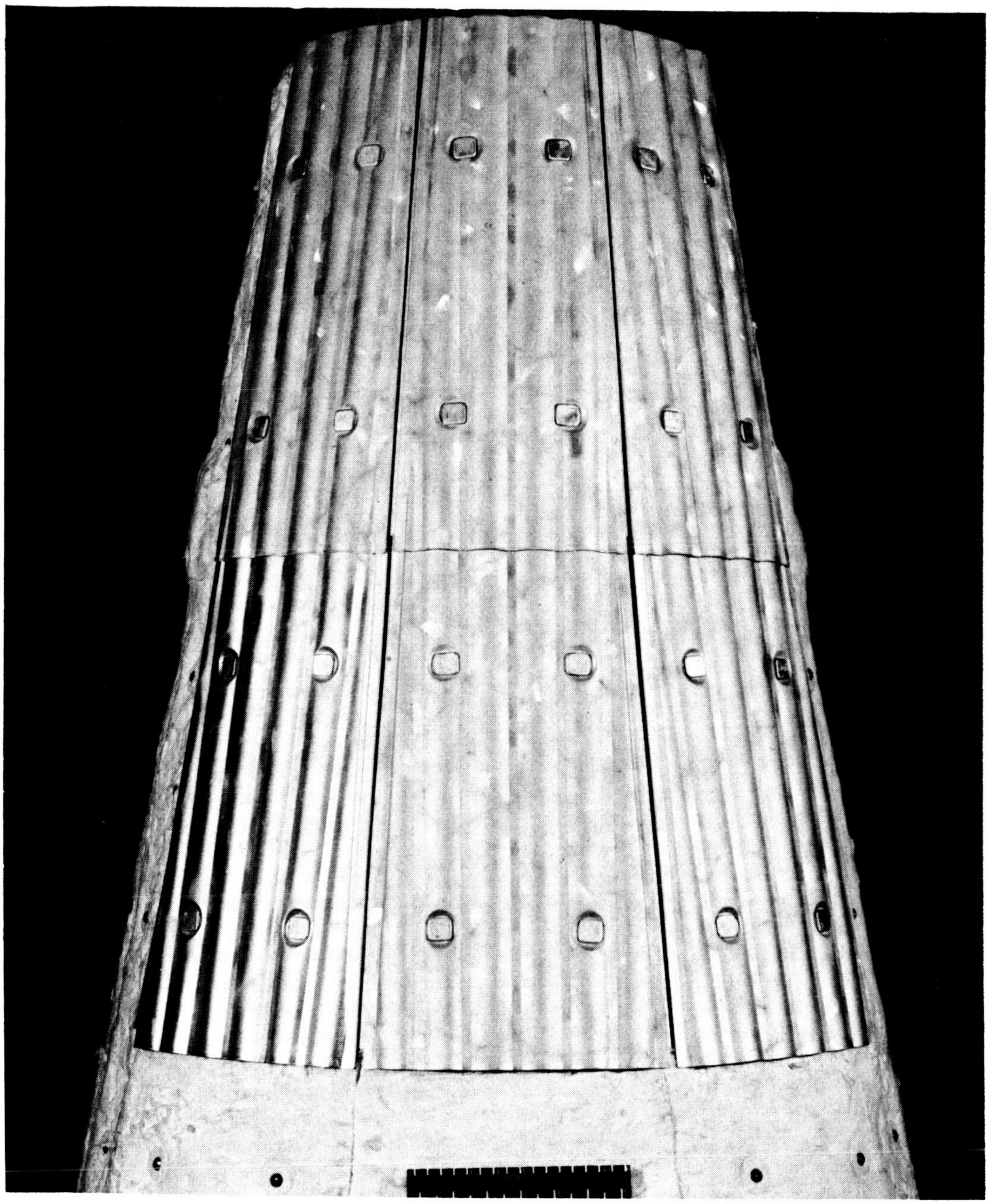

(a) Overall view. L-68-9469

Figure 7.- Curved shields, with Sn-27Al-5.5Mo coating, assembled on conical structure.

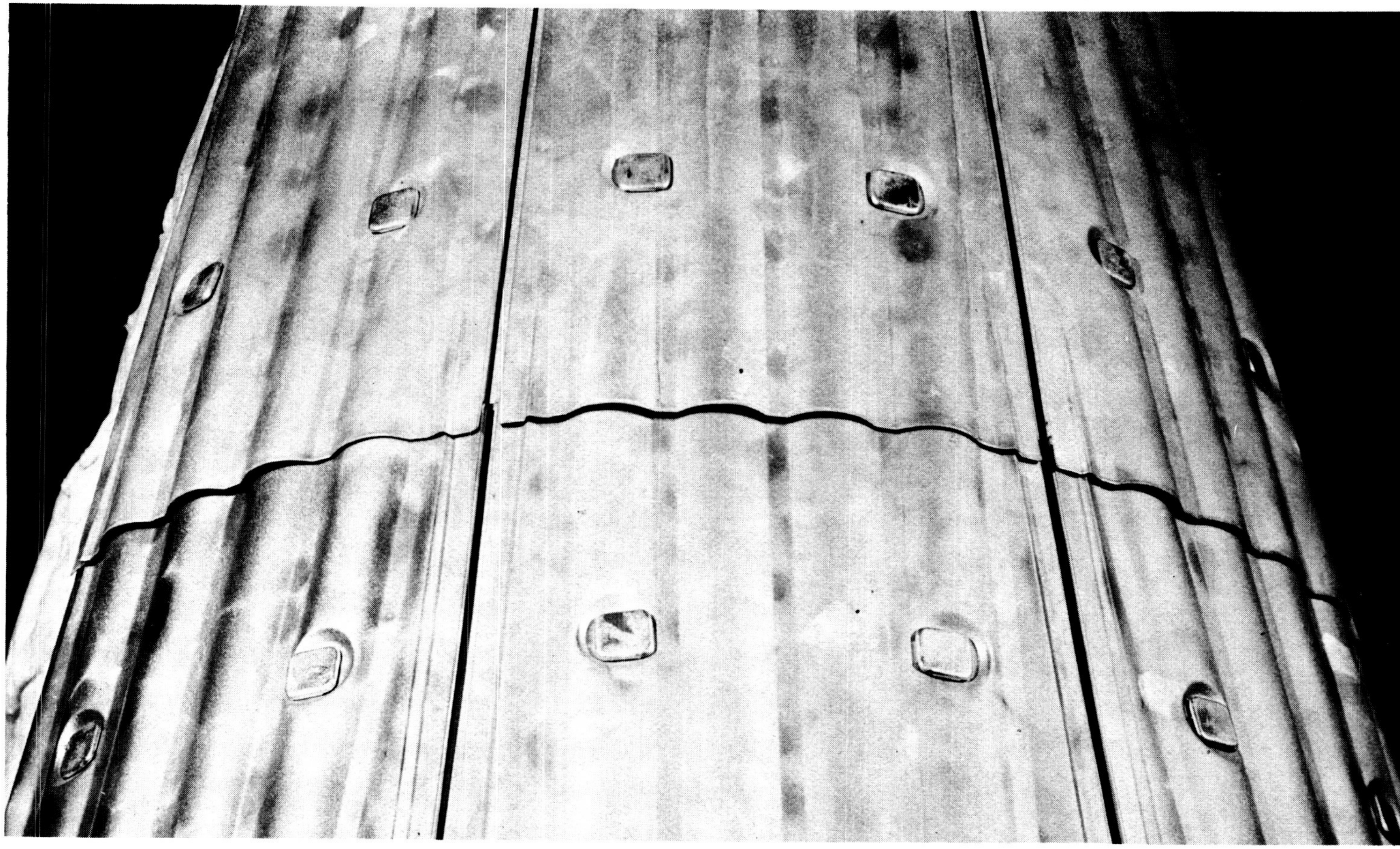

L-68-9472

(b) Closeup view of mating edges.

Figure 7.- Concluded.

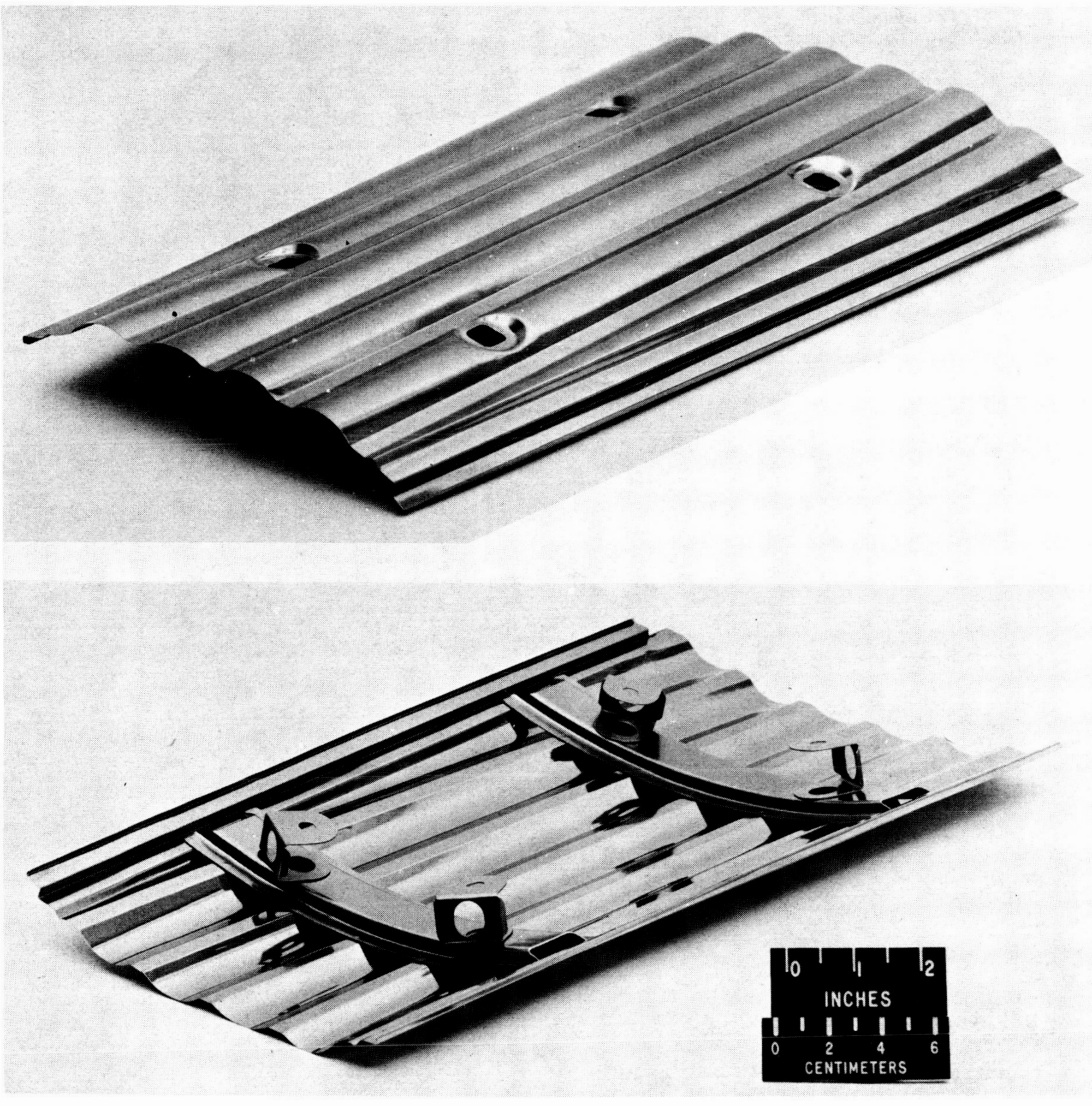

Figure 8.- Typical Ta-10W curved shield before coating. L-69-5087

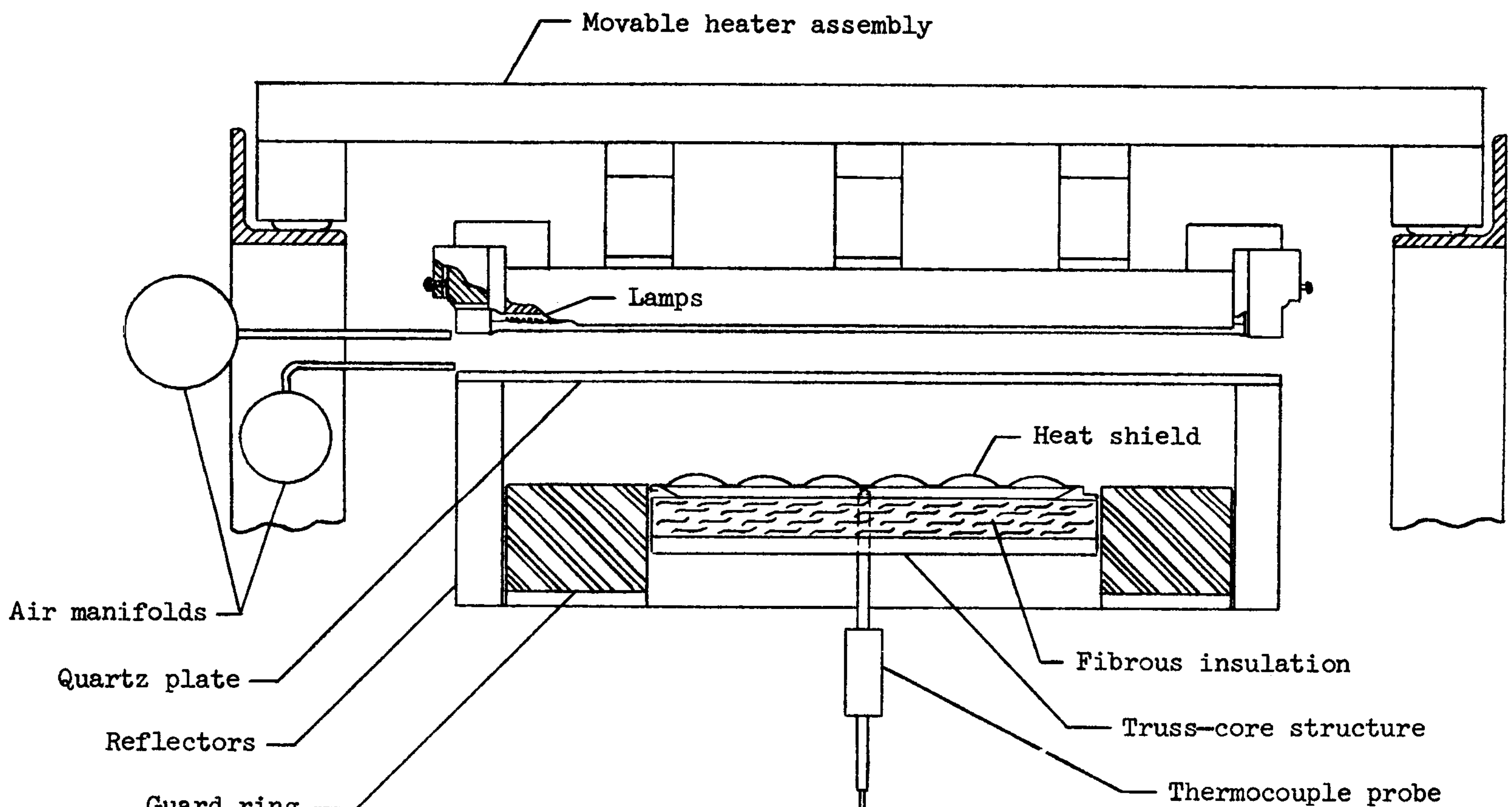

Figure 9.- Diagram of radiant-heating apparatus for testing flat heat-shield panels.

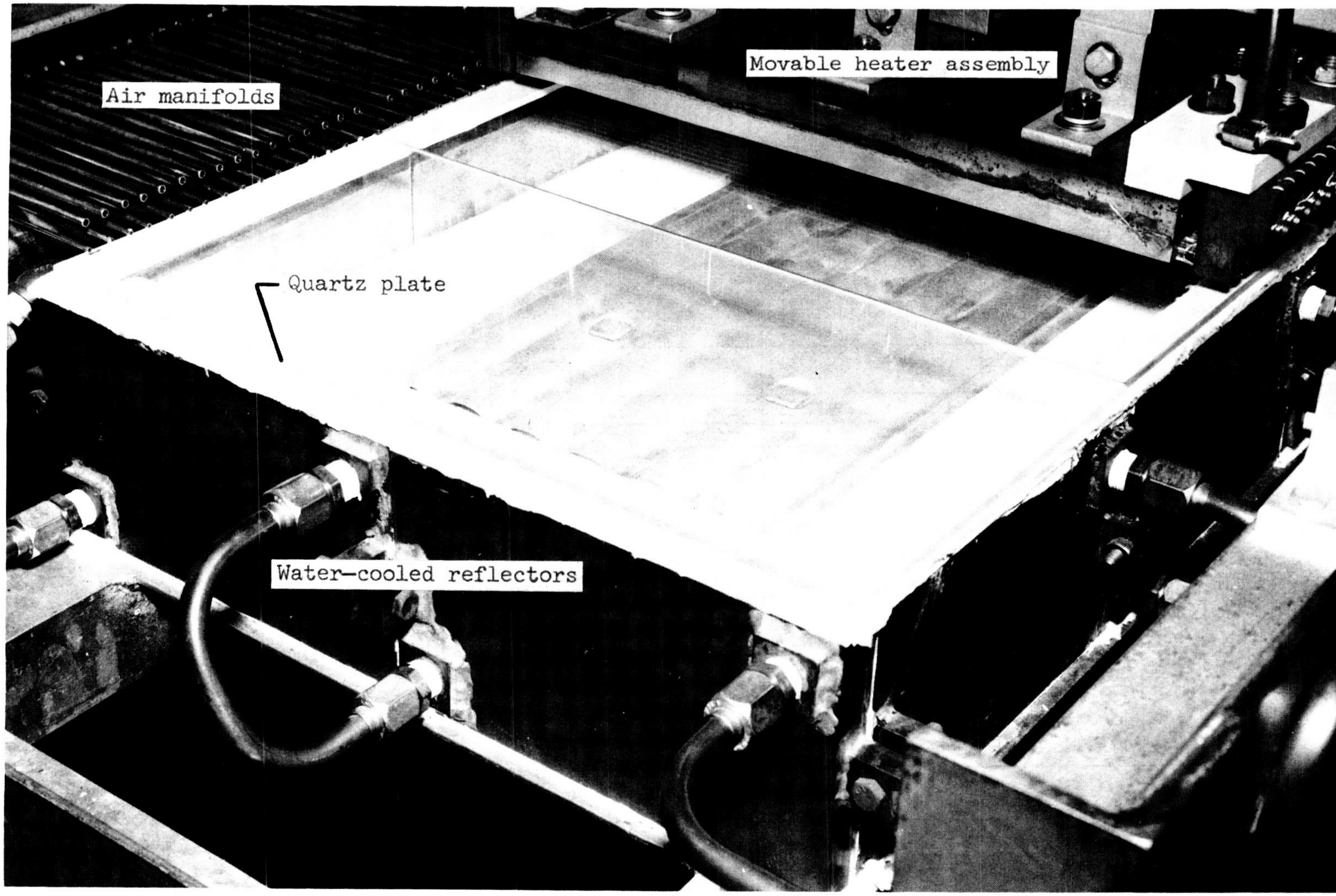

Figure 10.- Radiant-heating test setup with movable heater assembly in half-closed position.

L-68-1237.1

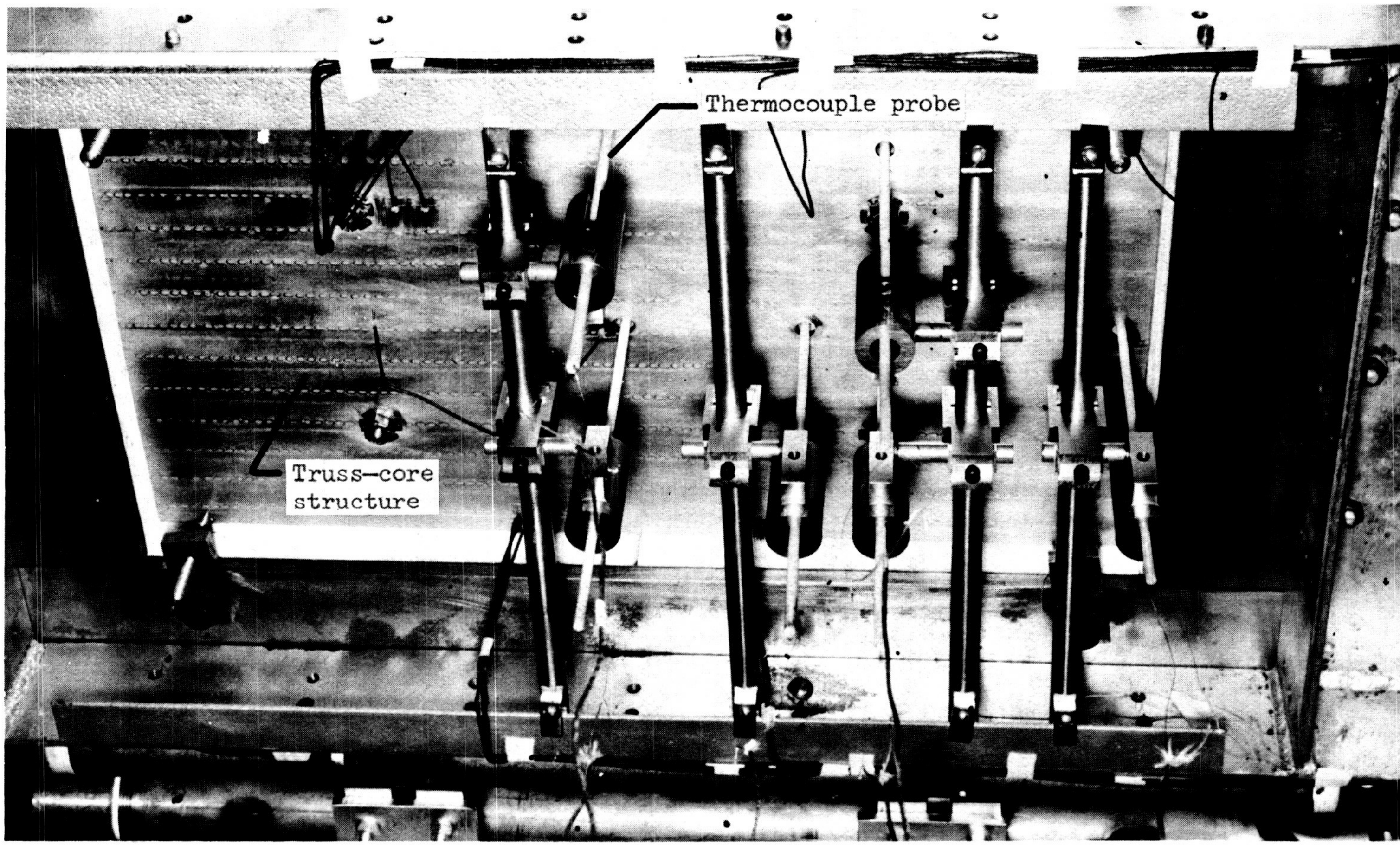

Figure 11.- Inside view of test enclosure showing thermocouple instrumentation for temperature-distribution tests on flat heat-shield panel. L-68-1234.1

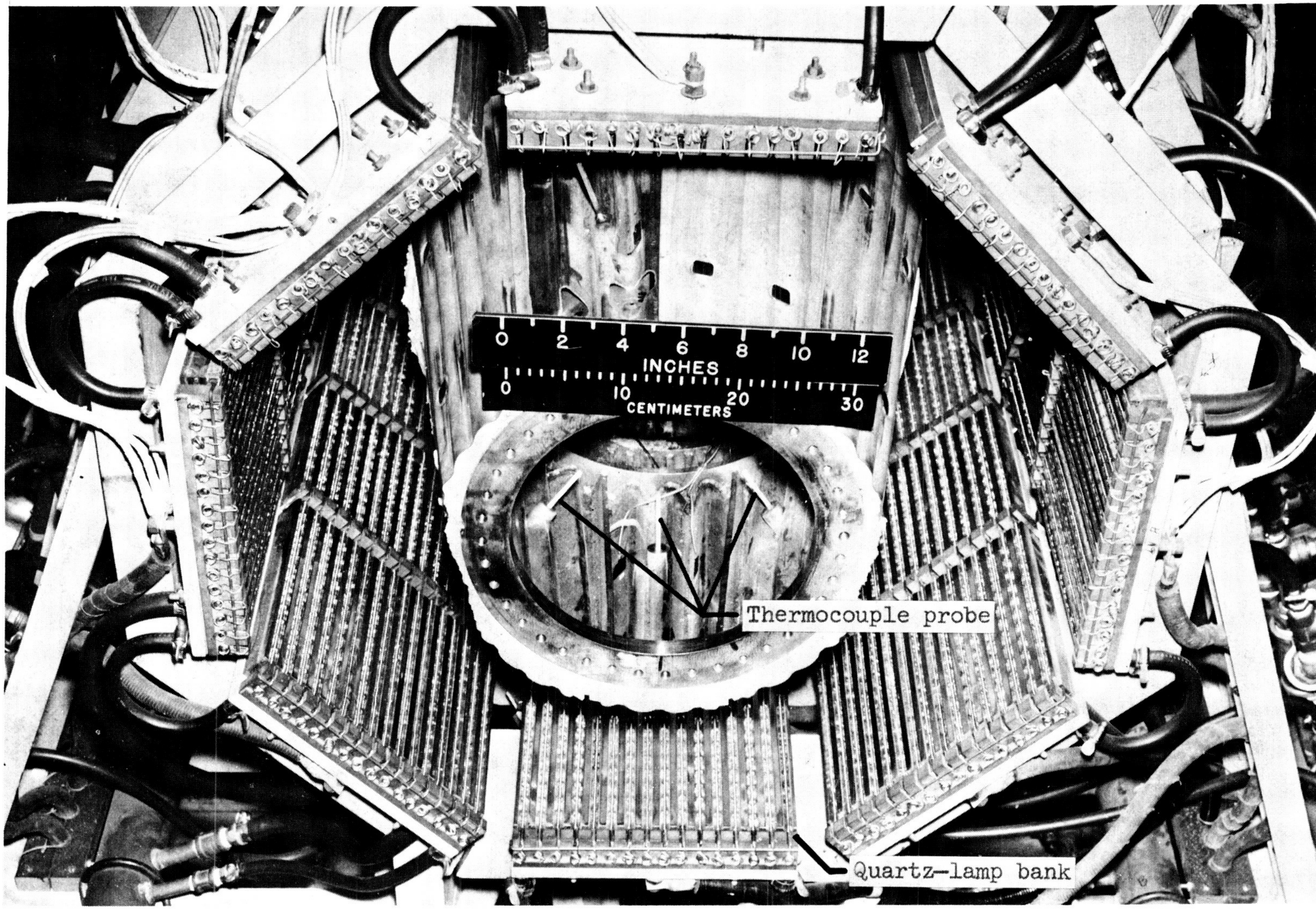

(a) Front view with lamps in test position.

L-68-9592.1

Figure 12.- Radiant-heating apparatus for testing of curved heat shields.

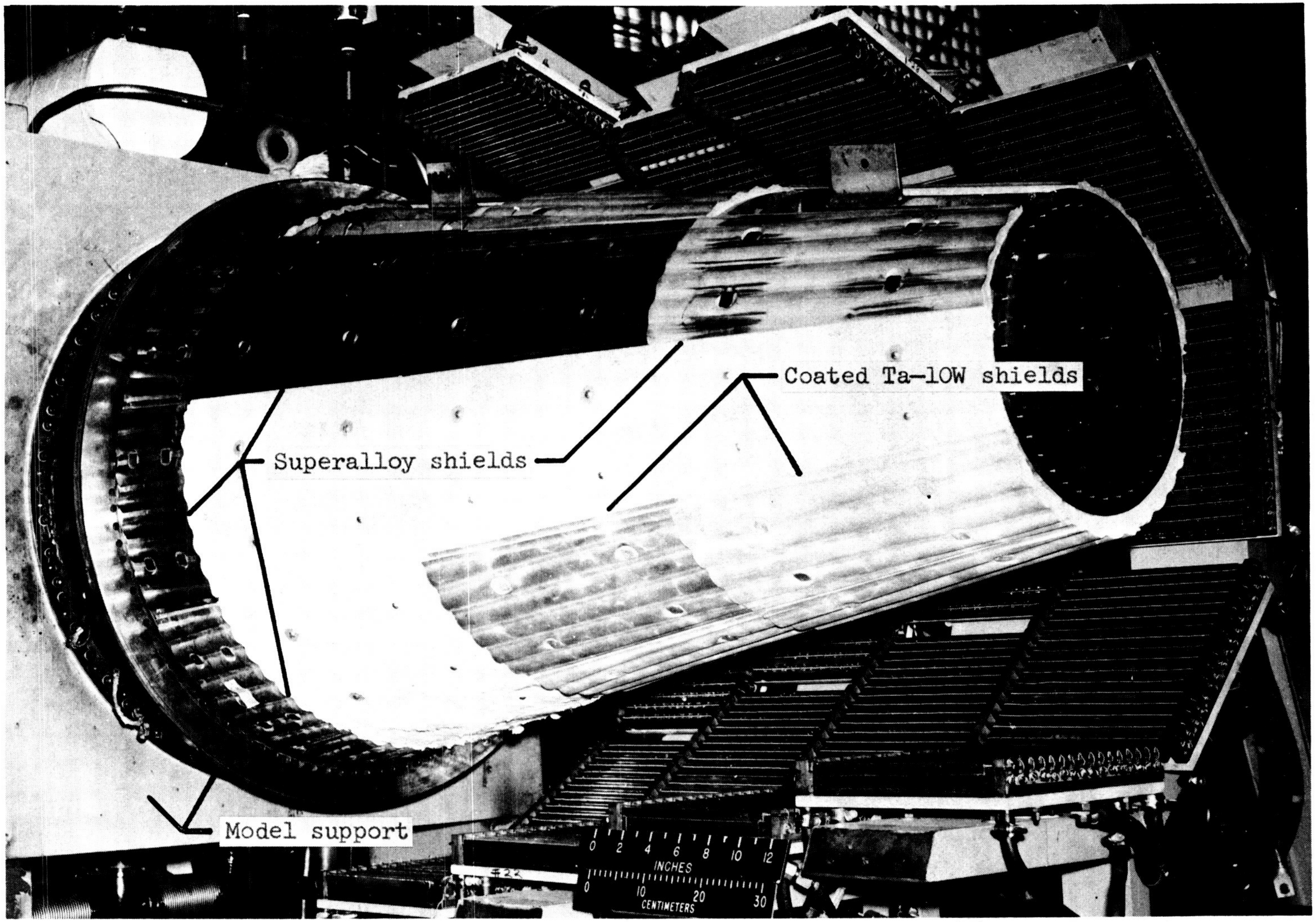

(b) Lamp section removed to show complete model and support. L-68-9595.1

Figure 12.- Concluded.

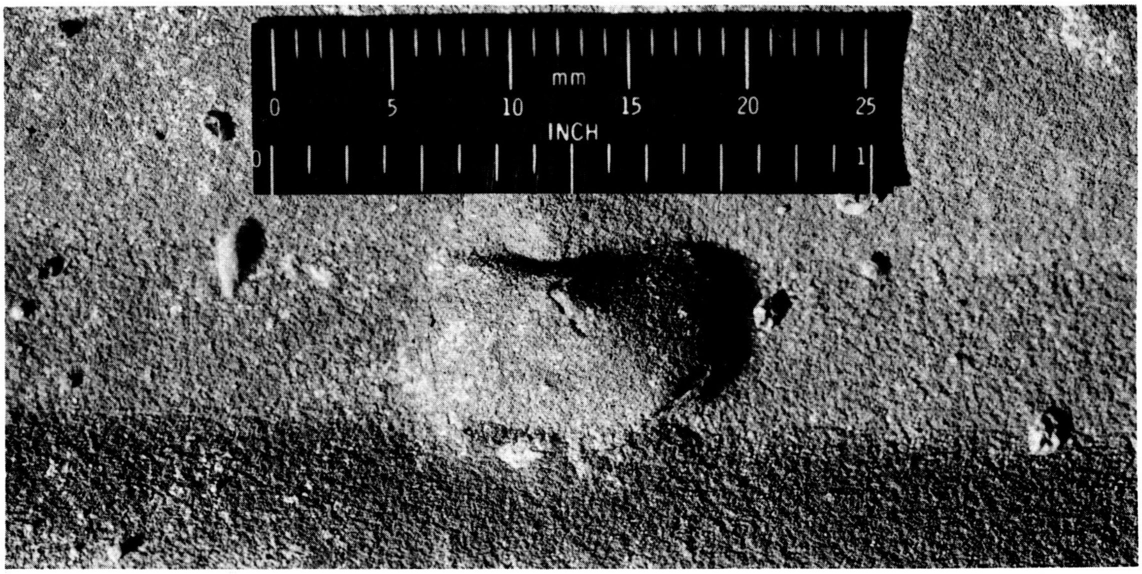

(a) Outer surface.

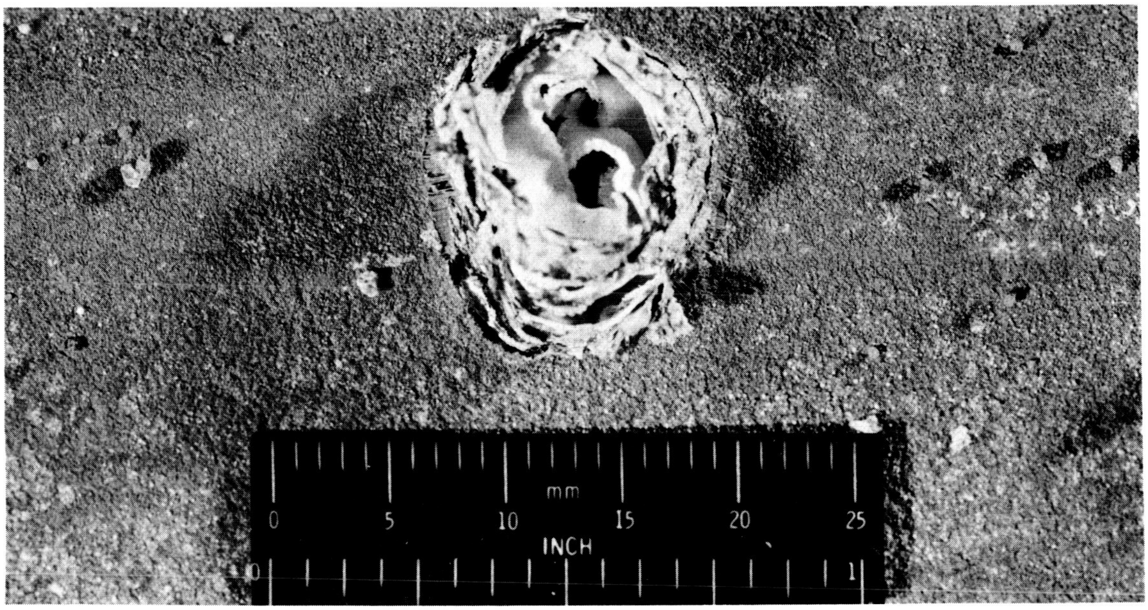

(b) Inner surface.

L-69-5088

Figure 13.- Detection of inner-surface coating failures on the corrugated skin by visual examination of the outer surface for the formation of coating blisters.

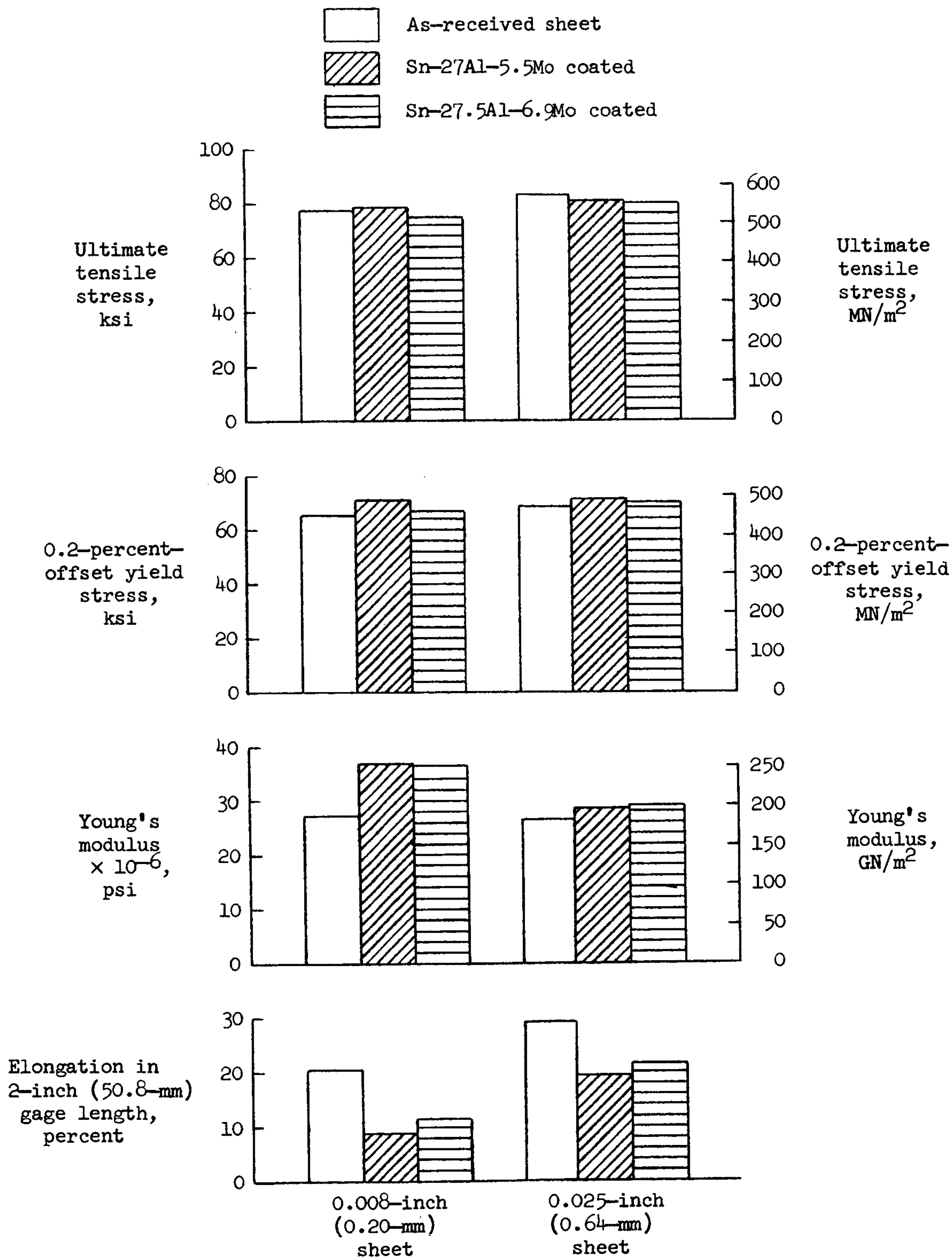

Figure 14.- Effect of aluminide coatings on room-temperature tensile properties of Ta-10W sheet based on as-received sheet thicknesses.

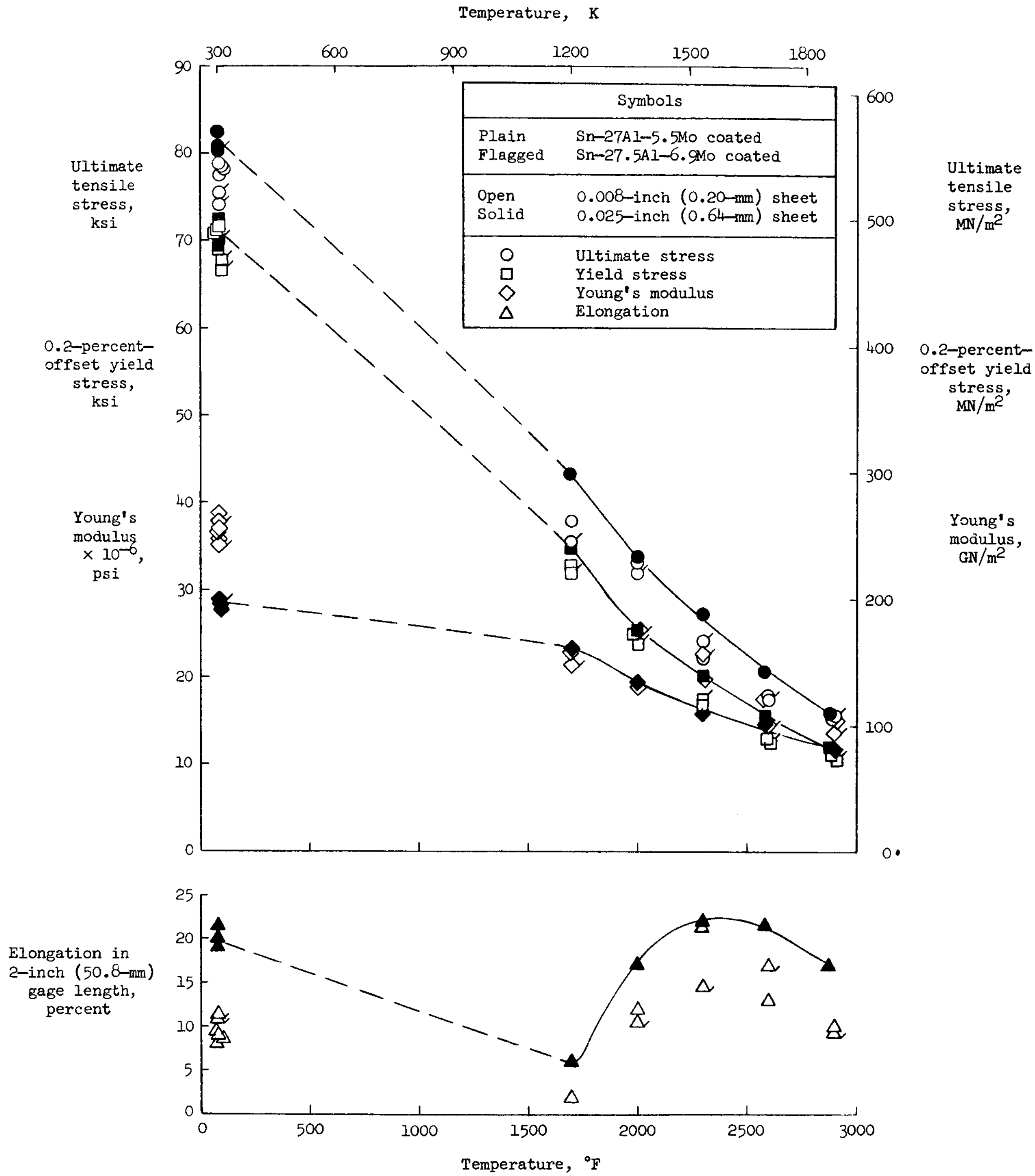

Figure 15.- Effect of temperature on tensile properties of Sn-27Al-5.5Mo and Sn-27.5Al-6.9Mo coated Ta-10W sheet based on as-received sheet thicknesses.

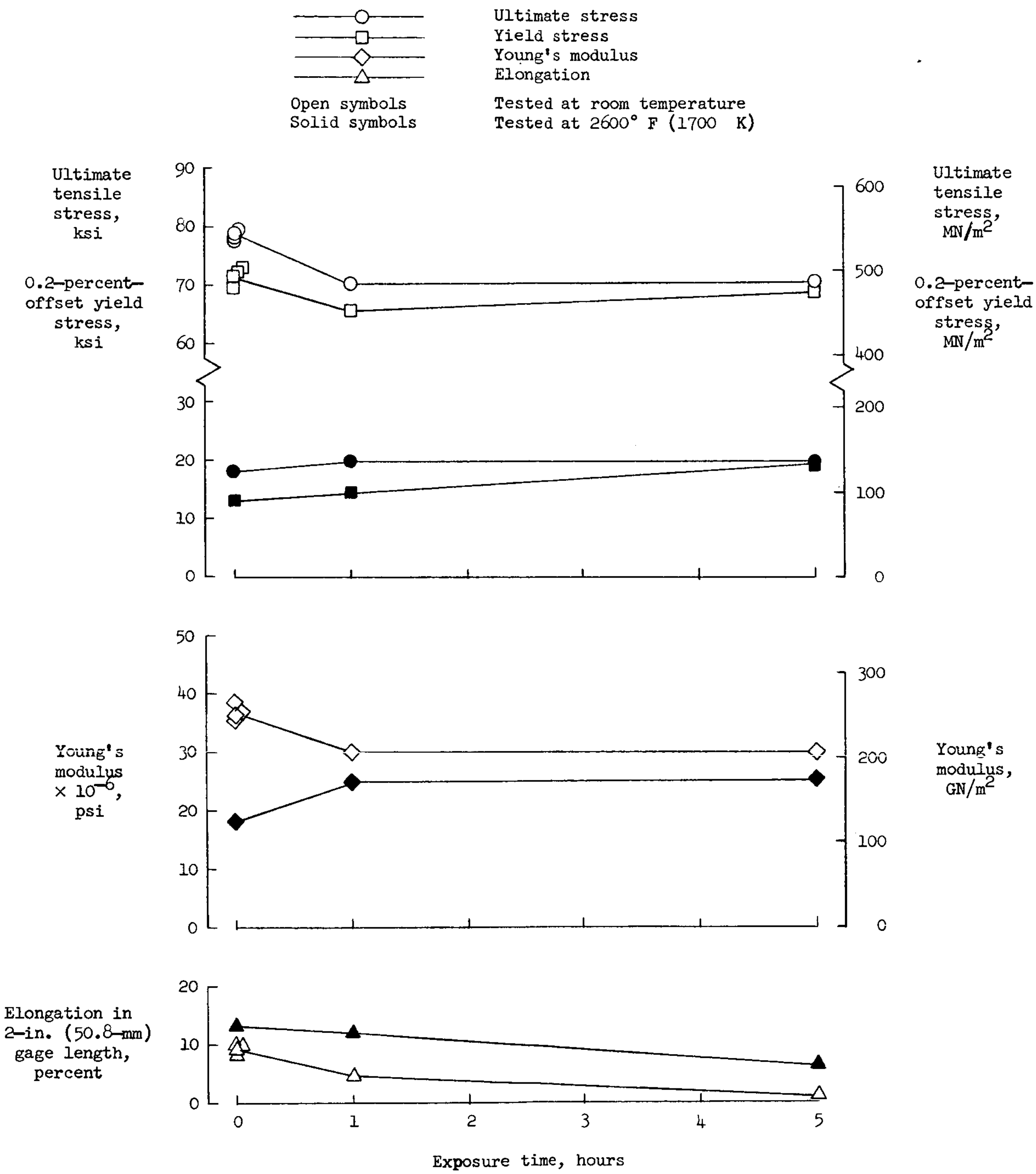

Figure 16.- Effect of time at elevated temperature (2600° F (1700 K)) on tensile properties on Sn-27Al-5.5Mo coating on 0.008-inch (0.20-mm) Ta-10W sheet.

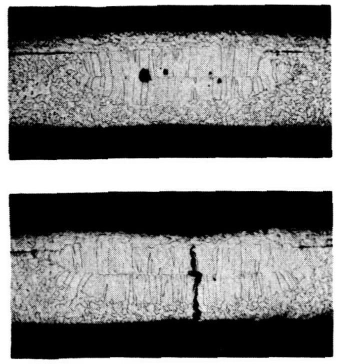

(a) Resistance spotwelds.

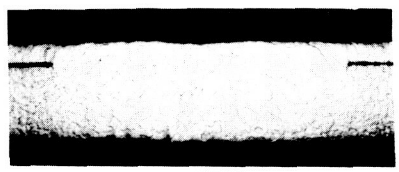

(b) Heliarc spotwelds.

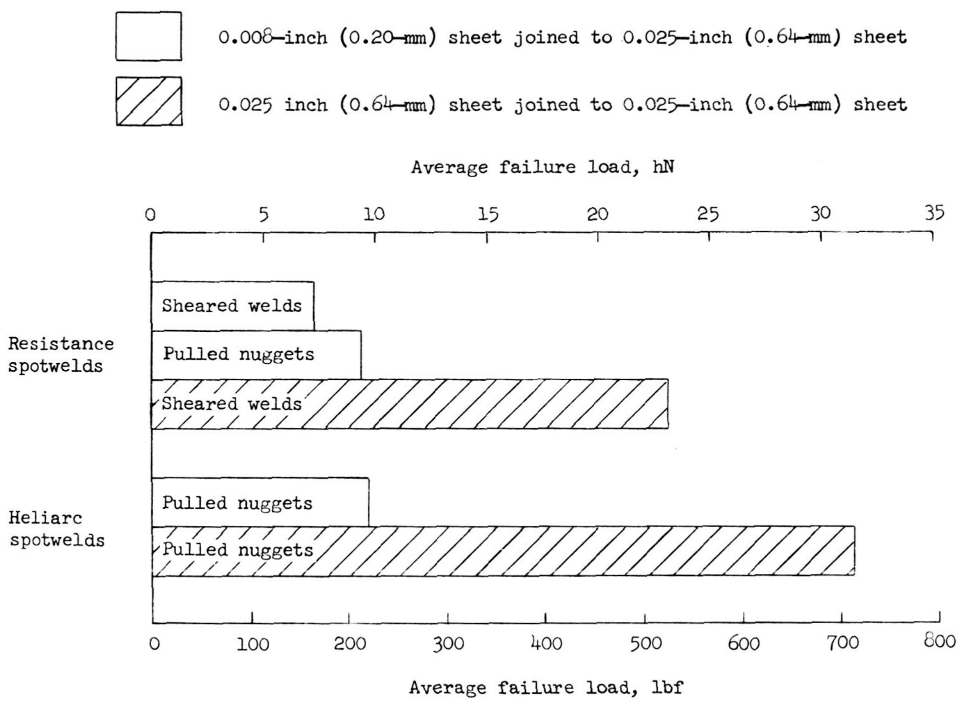

(c) Weld tensile-shear tests.

L-69-5089

Figure 17.- Cross-sectional views of resistance and heliarc spotwelds and results of weld tensile-shear tests on Ta-10W sheet specimens in the as-welded condition.

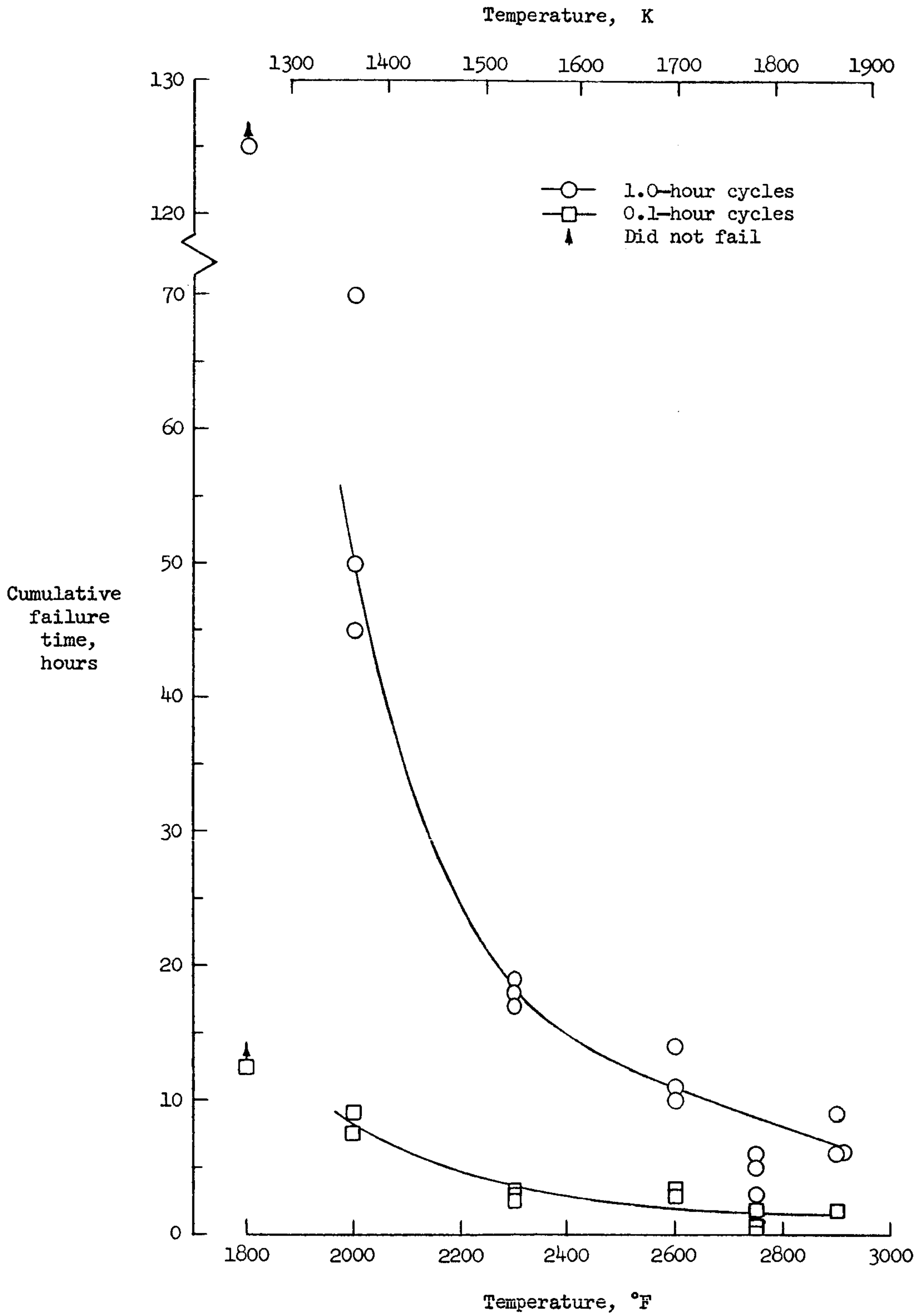

Figure 18.- Effect of temperature and cyclic exposure on coating life of Sn-27Al-5.5Mo coated Ta-10W coupons under static oxidation.

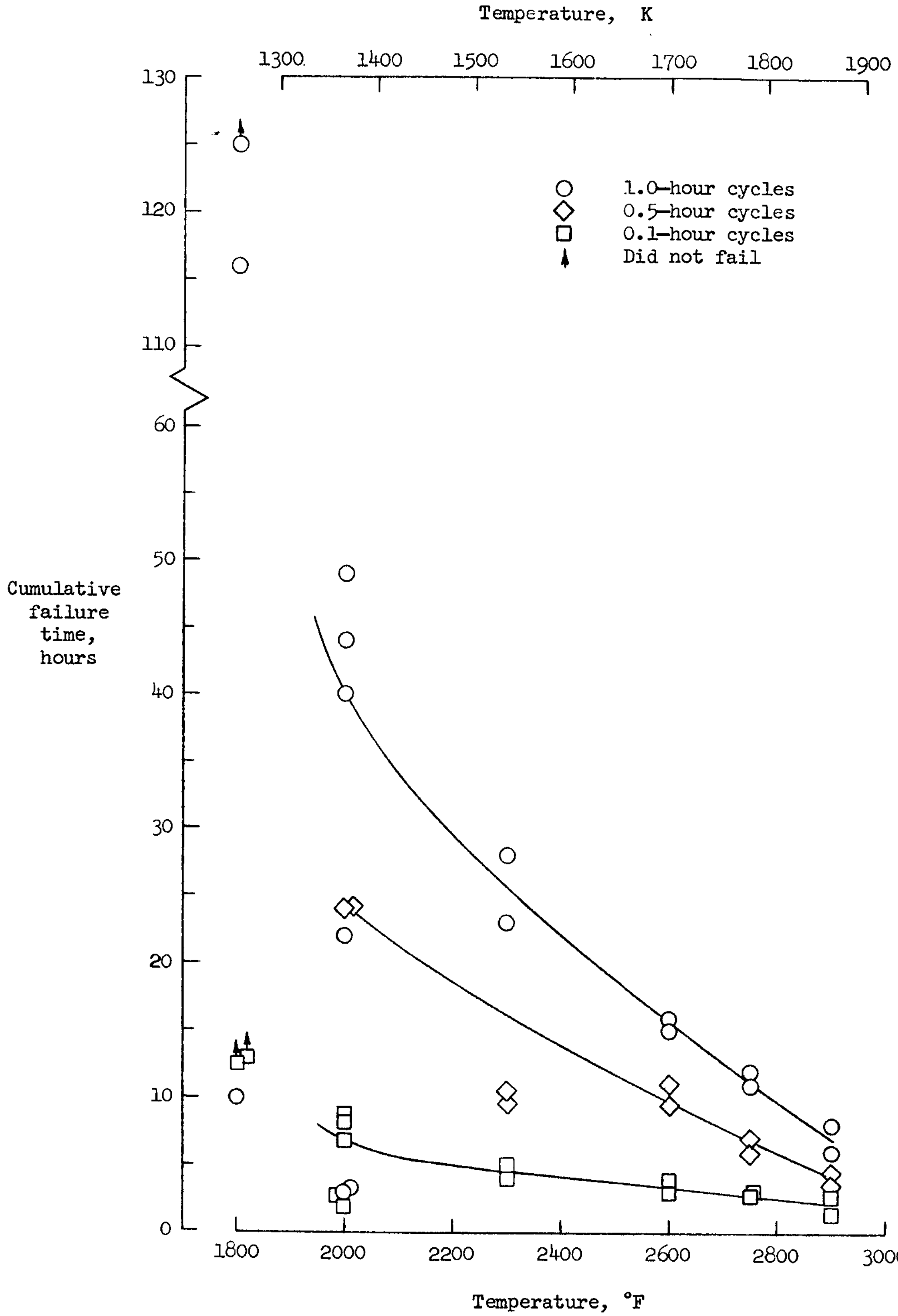

Figure 19.- Effect of temperature and cyclic exposure on coating life of Sn-27.5Al-6.9Mo coated Ta-10W coupons under static oxidation.

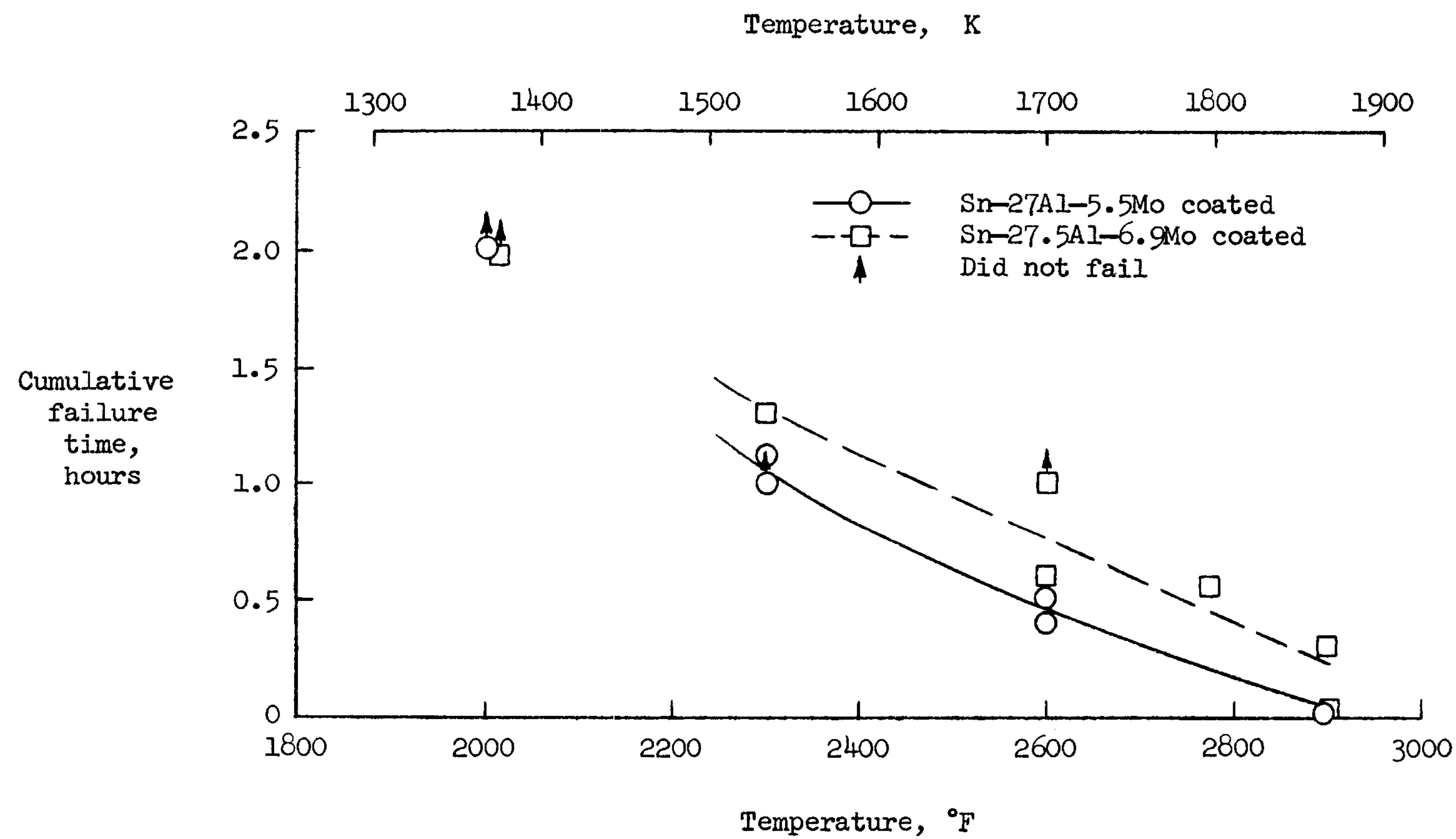

Figure 20.- Results of arc-jet tests on aluminide-coated Ta-10W leading-edge specimens under 0.1-hour cyclic exposures.

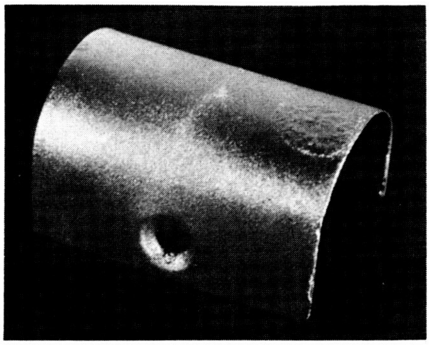

(a) As-coated.

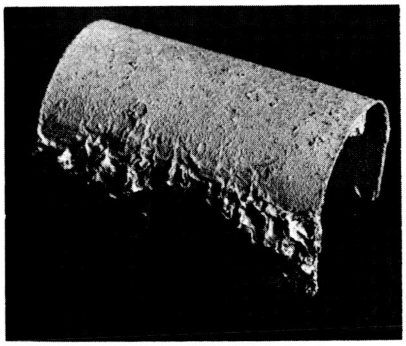

(b) After 1 cycle.

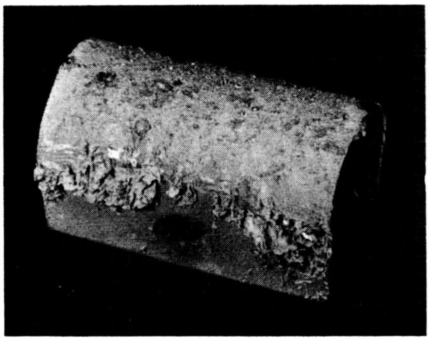

(c) After 5 cycles.

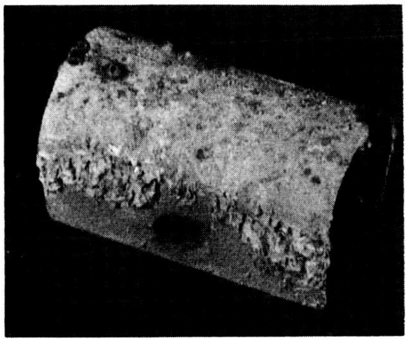

(d) After 6 cycles.

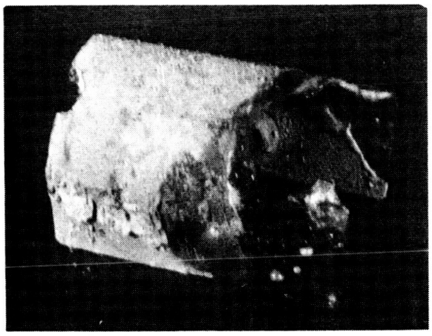

(e) After ignition at start of 7th cycle. L-69-5090

Figure 21.- Tantalum-alloy leading edge coated with Sn-27.5Al-6.9Mo before and after 0.1-hour exposures at 2900° F (1865 K) in subsonic airstream.

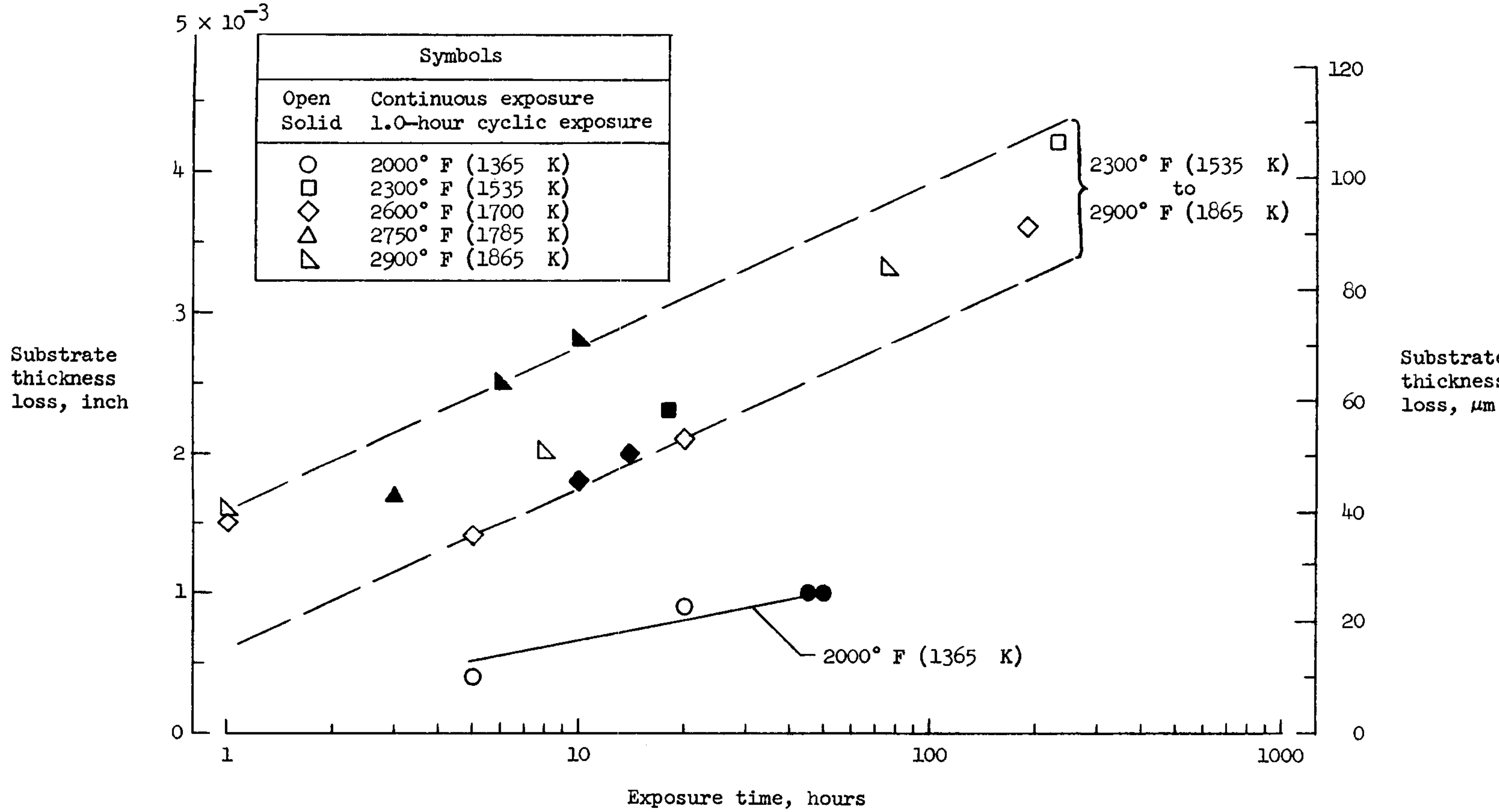

Figure 22.- Variation in substrate thickness loss with exposure time for Sn-27Al-5.5Mo coated Ta-10W sheet based on as-coated substrate thickness of 0.0075-inch (190 μm).

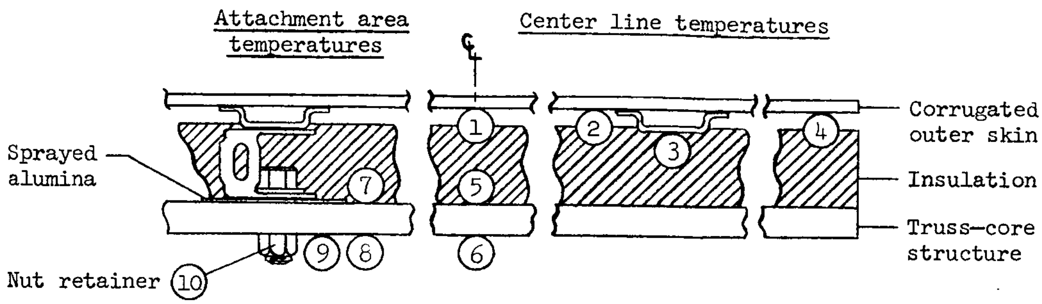

(a) Thermocouple locations.

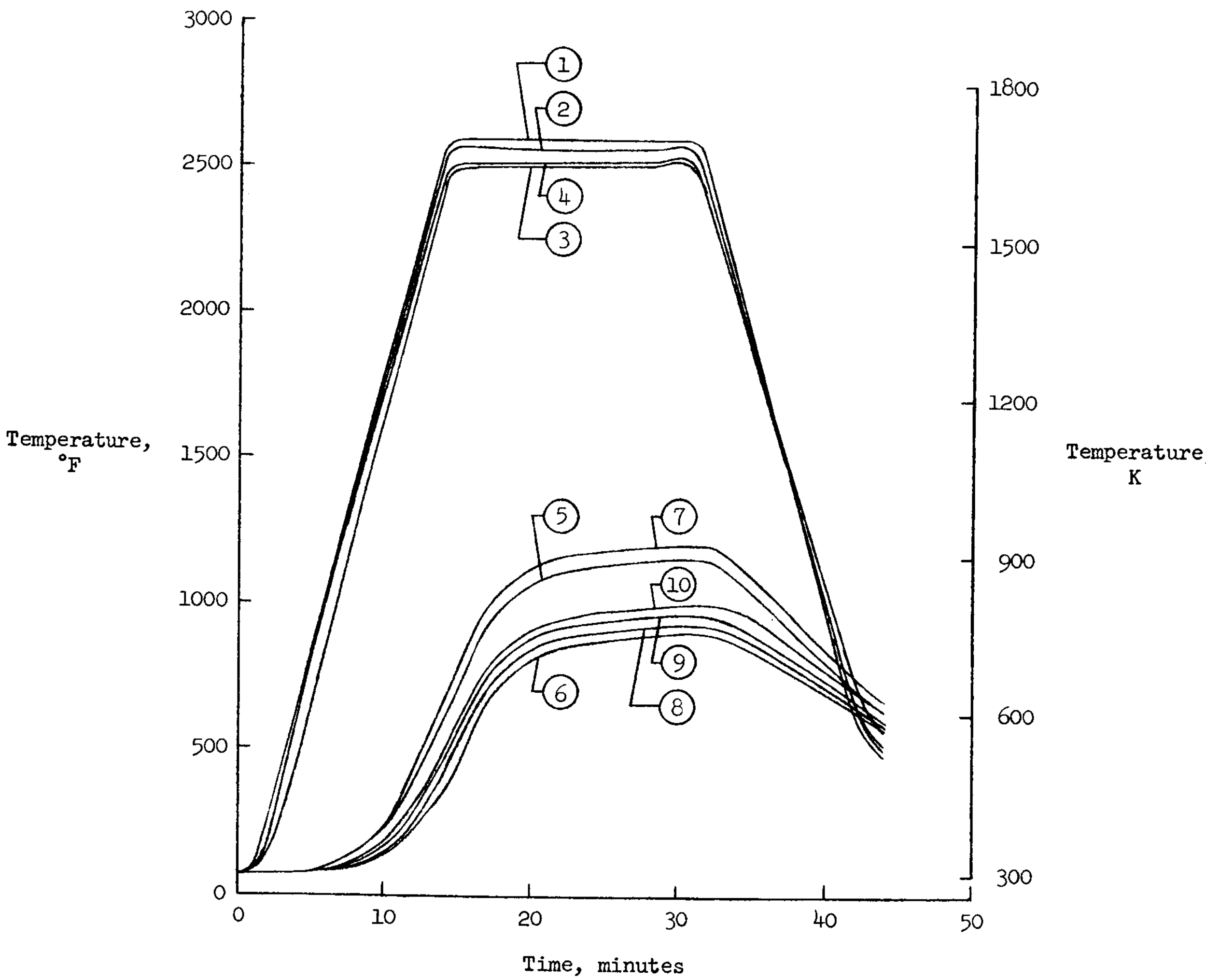

(b) Temperature distribution for 2600° F (1700 K) profile.

Figure 23.- Temperature distributions through heat-shield panel 1 for 2600° F (1700 K) and 2900° F (1865 K) profiles. Circled numbers denote thermocouple locations.

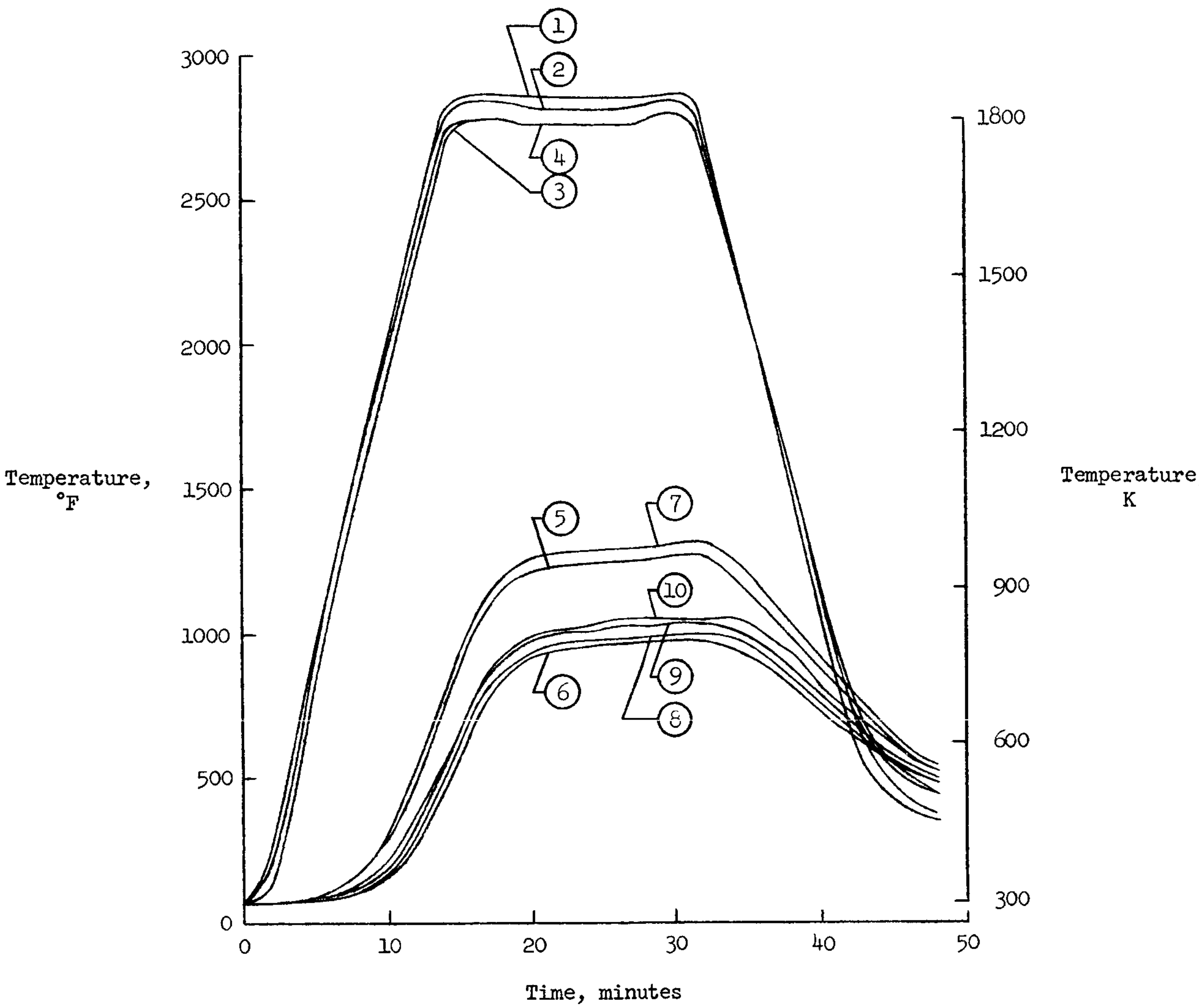

(c) Temperature distribution for 2900° F (1865 K) profile.

Figure 23.- Concluded.

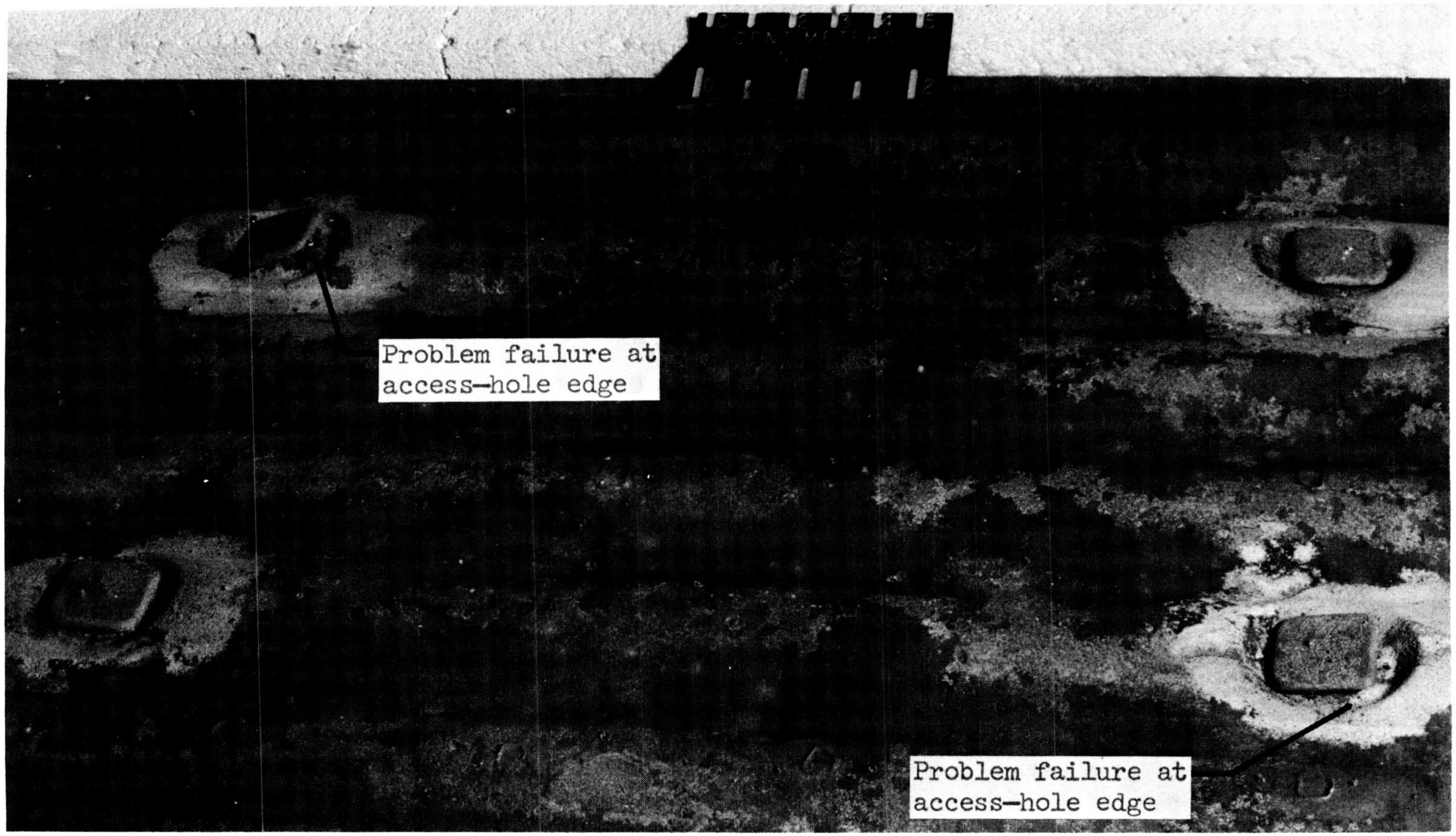

(a) After 4 cycles showing problem-area failures only.

L-68-2048.1

Figure 24.- Coating failures on the Sn-27Al-5.5Mo coated shield (shield 2) after cyclic exposures to 2600^{0} F (1700 K).

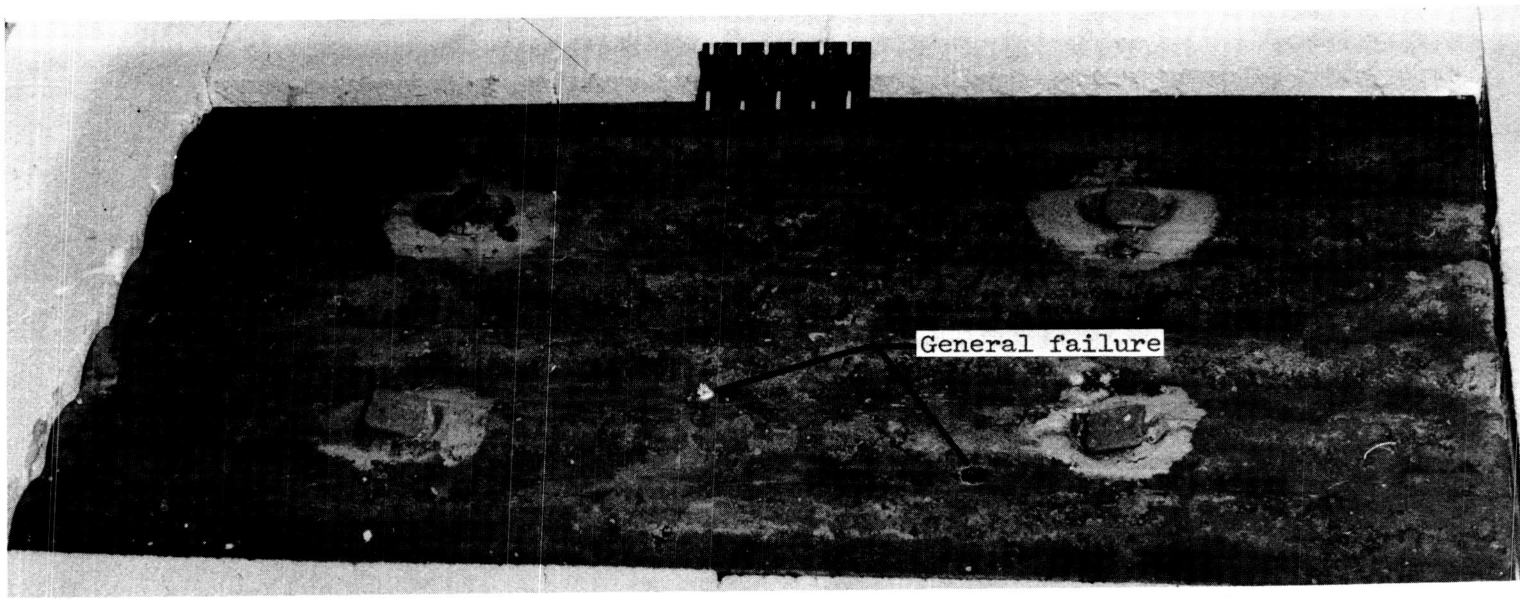

L-68-2055.1

(b) After 9 cycles showing general and problem failures.

Figure 24.- Concluded.

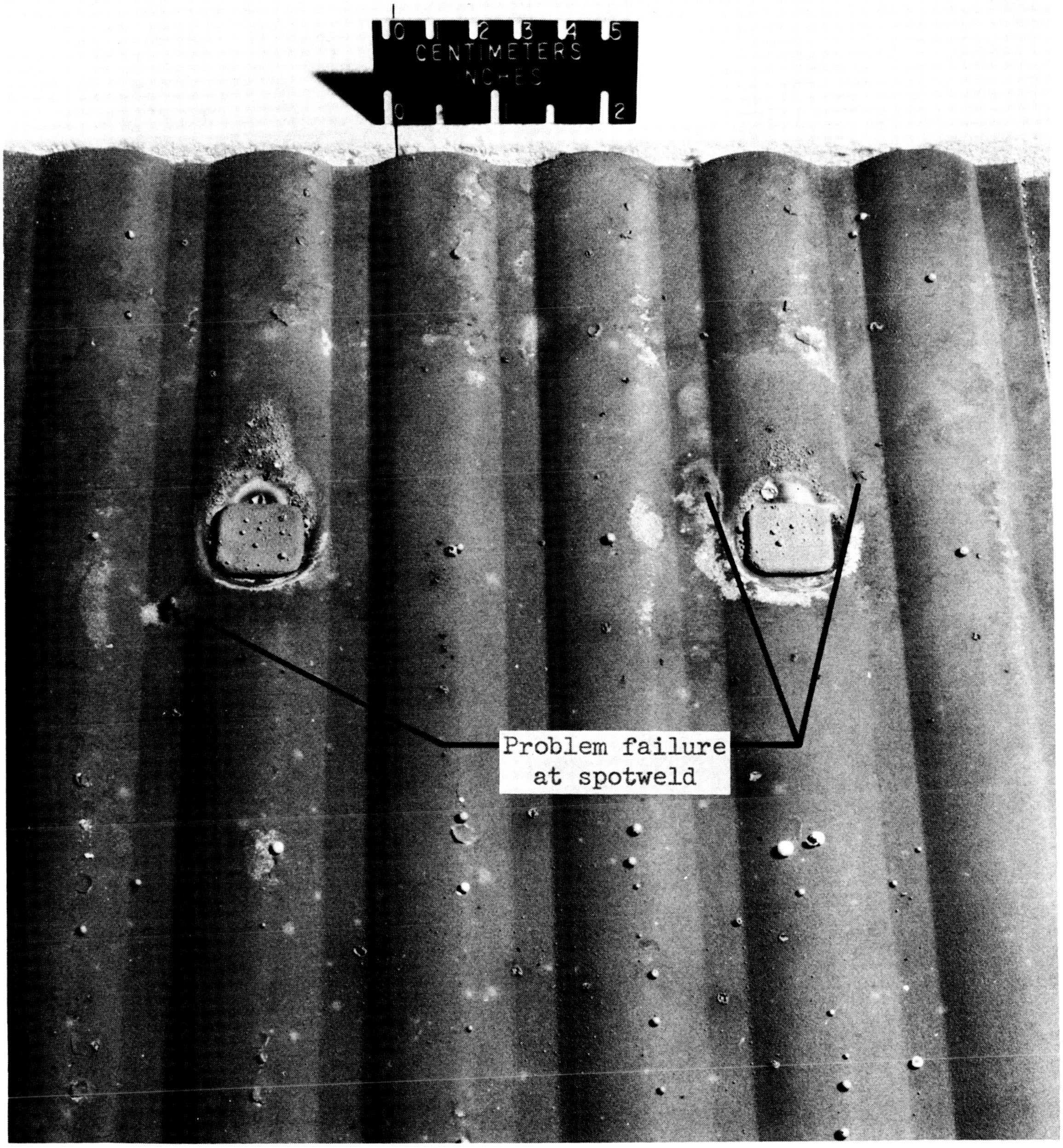

(a) After 4 cycles showing problem failures only. L-68-2673.1

Figure 25.- Coating failures on spotwelded tantalum-alloy shield 3 with Sn-27.5Al-6.9Mo coating after cyclic exposures to 2600° F (1700 K).

(b) After 11 cycles showing general and problem failures. L-68-2788.1

Figure 25.- Concluded.

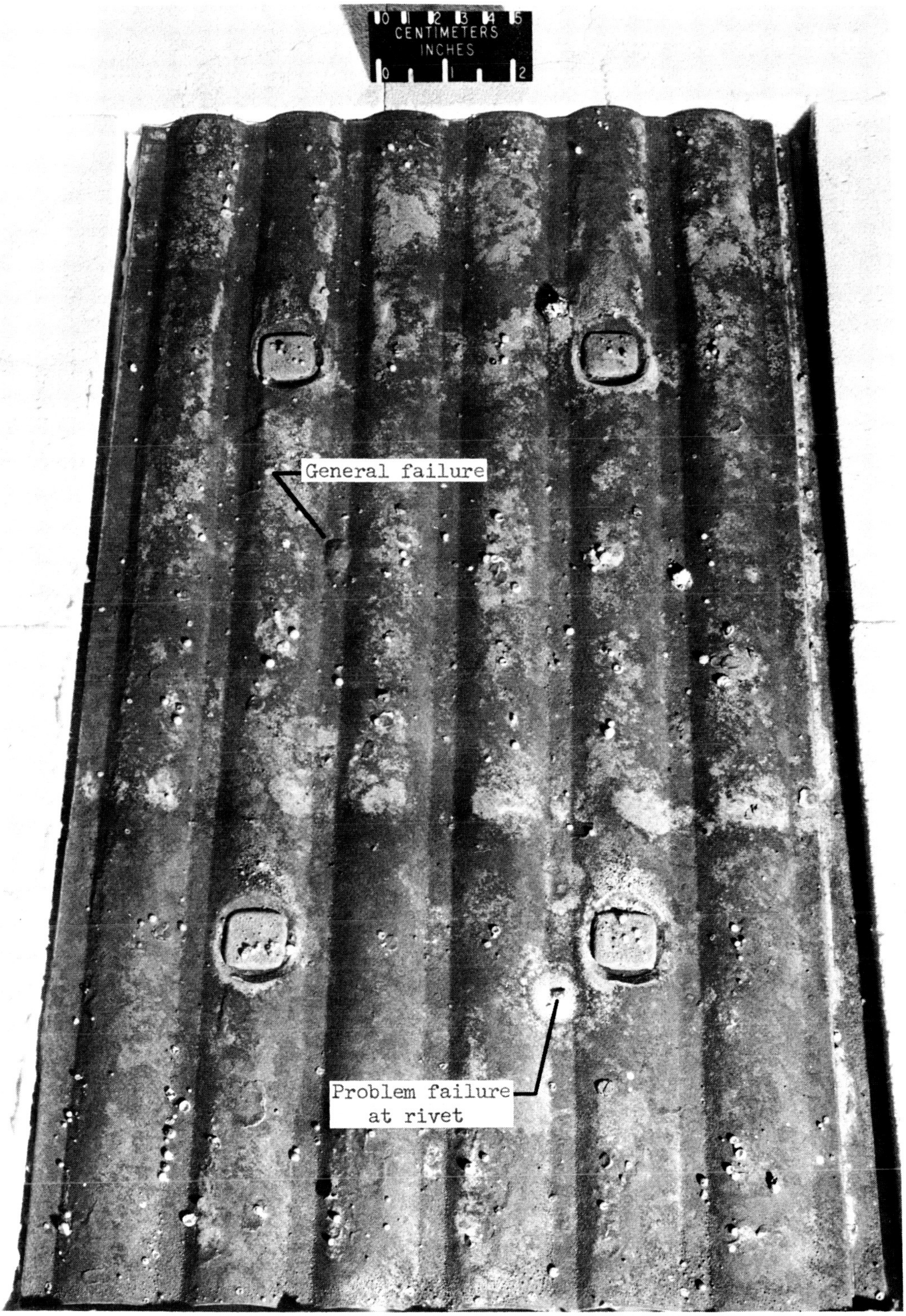

L-68-3325.1

Figure 26.- Coating failures on riveted tantalum-alloy shield (shield 5) with Sn-27.5Al-6.9Mo coating after 12 cycles to 2600° F (1700 K).

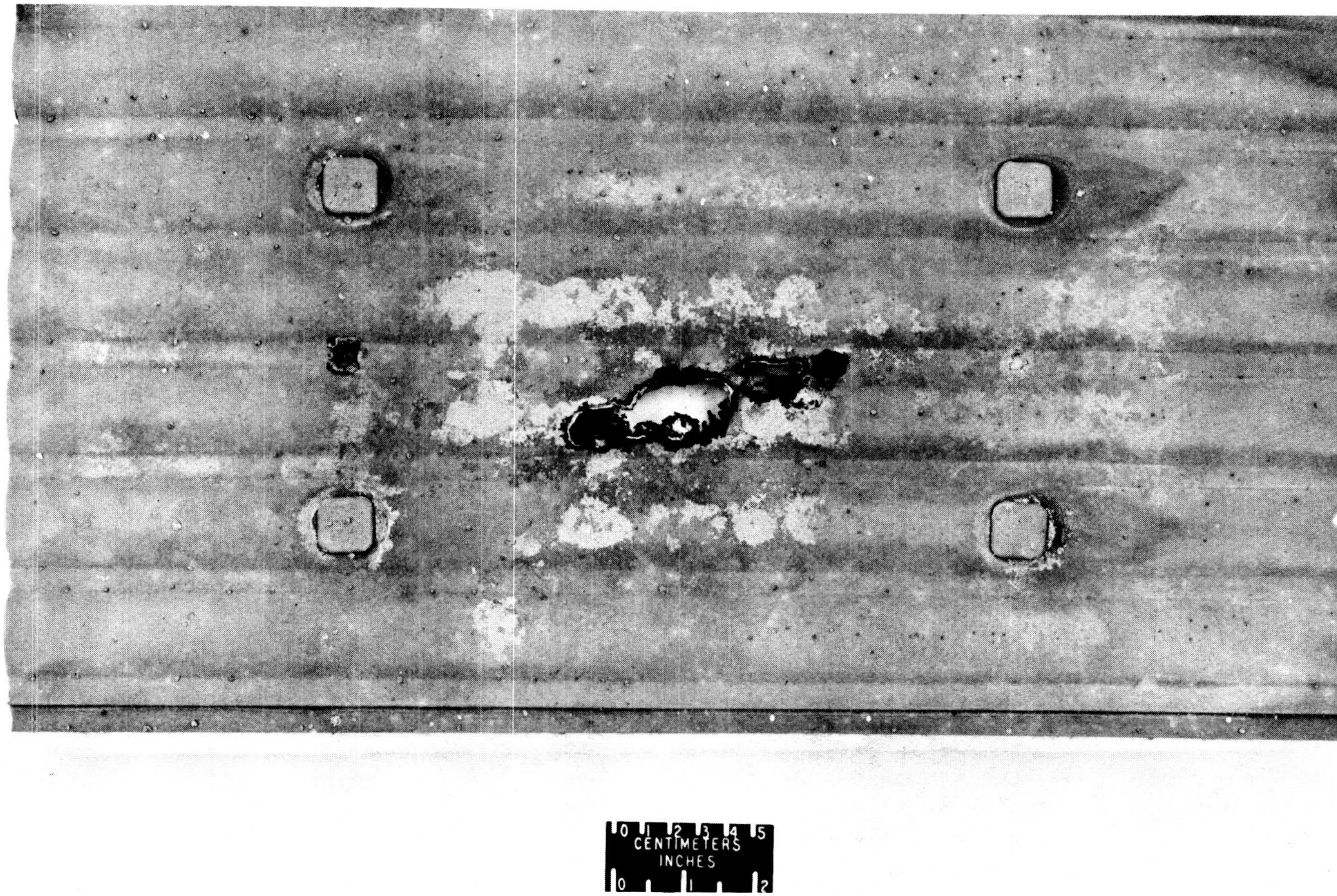

(a) Outer surface appearance.

L-68-5876

Figure 27.- Failures on Sn-27.5Al-6.9Mo coated Ta-10W shield after 3 cycles at 2900° F (1865 K).

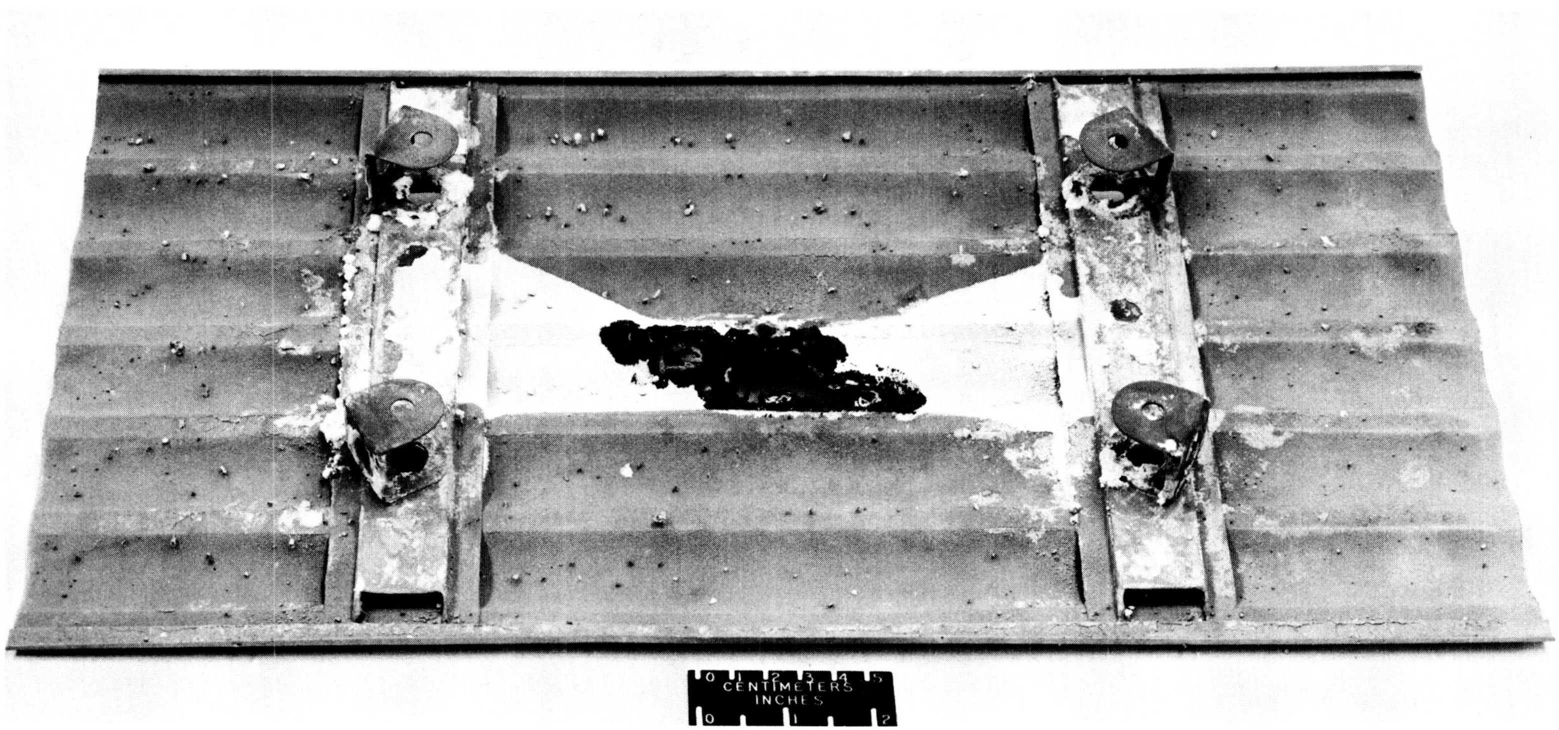

L-68-5880

(b) Inner surface with white deposit of αAl_2O_3.

Figure 27.- Continued.

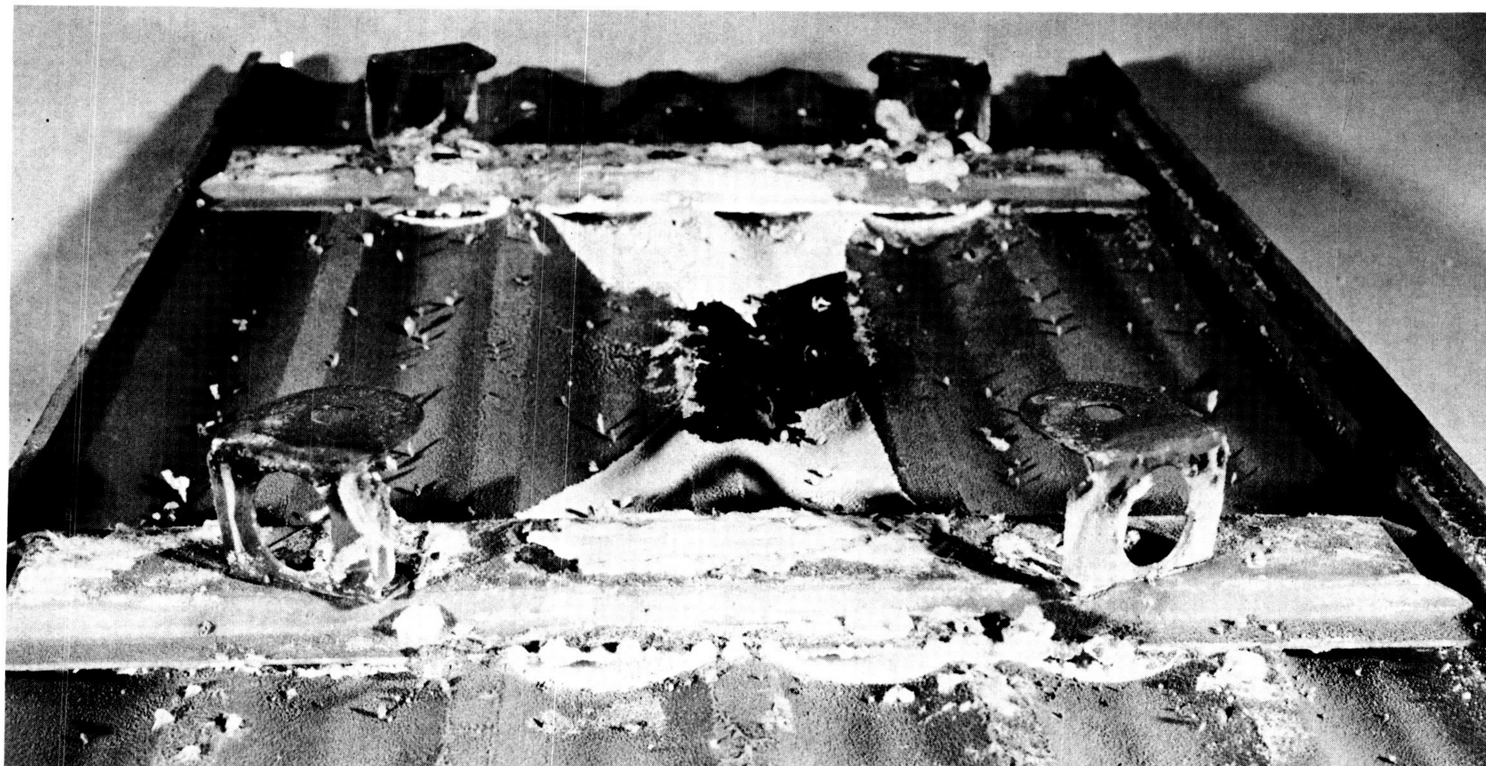

L-68-5879

(c) Deposit of αAl_2O_3 under hat sections.

Figure 27.- Concluded.

Symbols	
Open	General failures
Solid	Problem failures
— — — — —	Life estimated from coupon data
○	Welded heat shields
□	Riveted heat shield

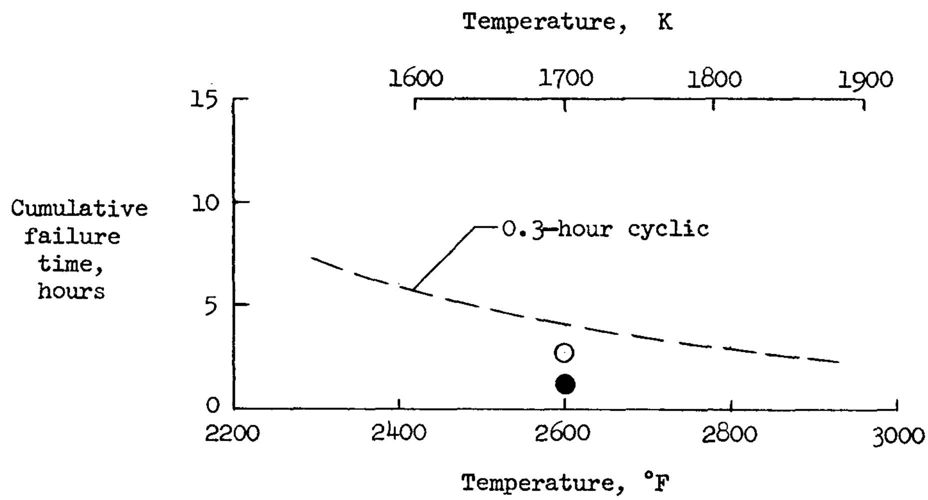

(a) Sn-27Al-5.5Mo coating.

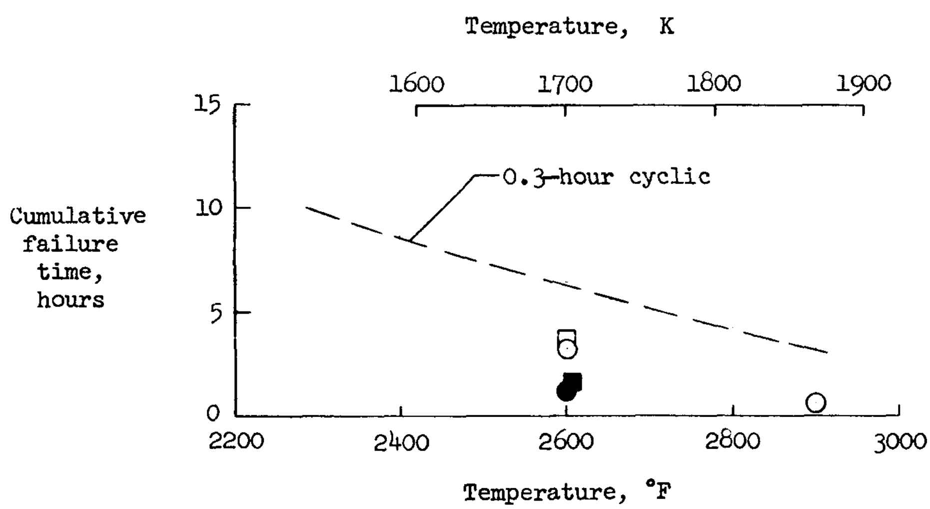

(b) Sn-27.5Al-6.9Mo coating.

Figure 28.- Comparison of aluminide-coating life on tantalum-alloy heat shields with life estimated from small coupons.

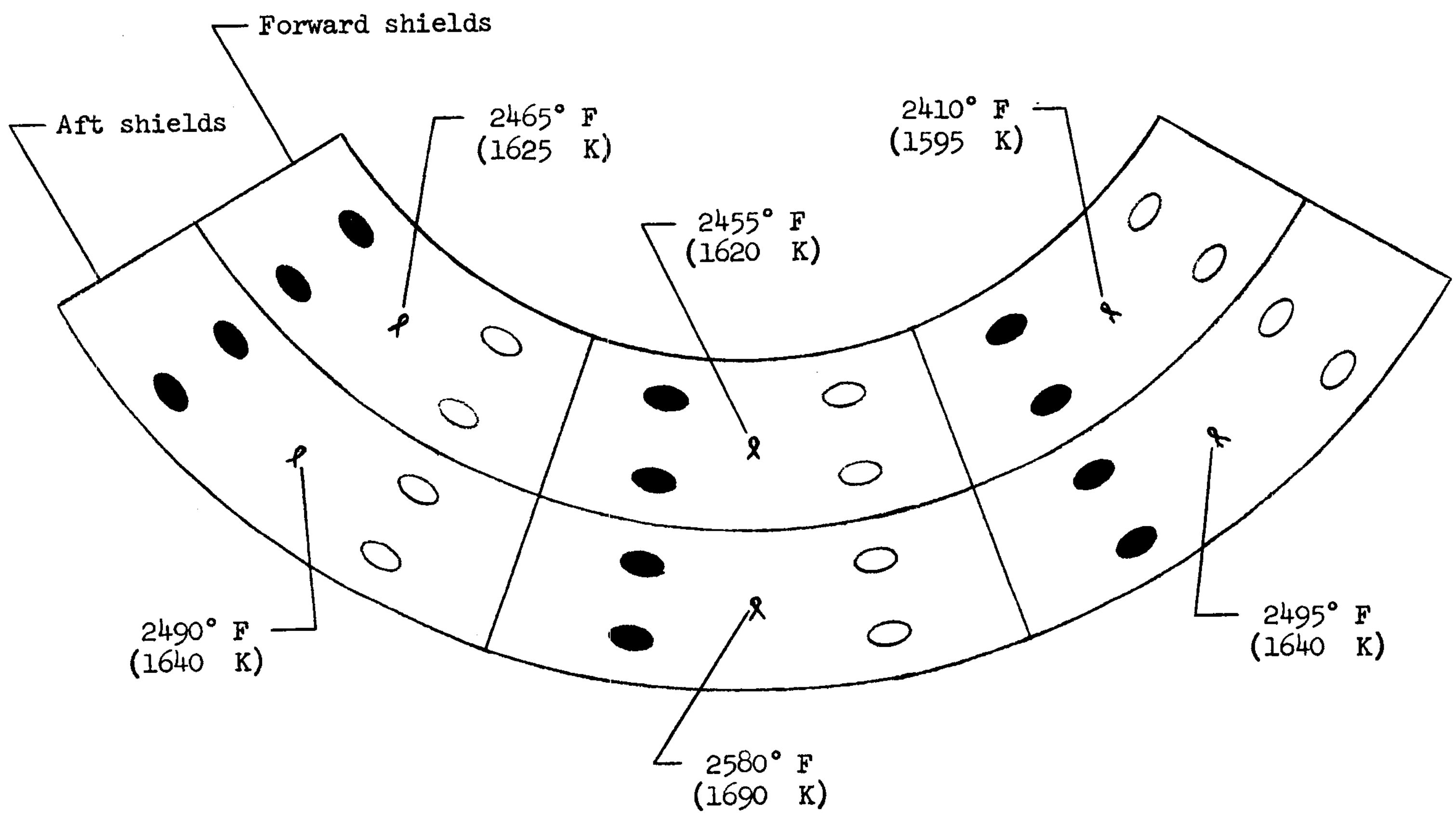

Denote heat-shield plugs
Open symbol — Inserted and removed with hot-air gun
Solid symbol — Inserted and removed at room temperature

Figure 29.- Measured heat-shield temperatures during 0.1-hour hold period for programed 2600° F (1700 K) profile cycles.

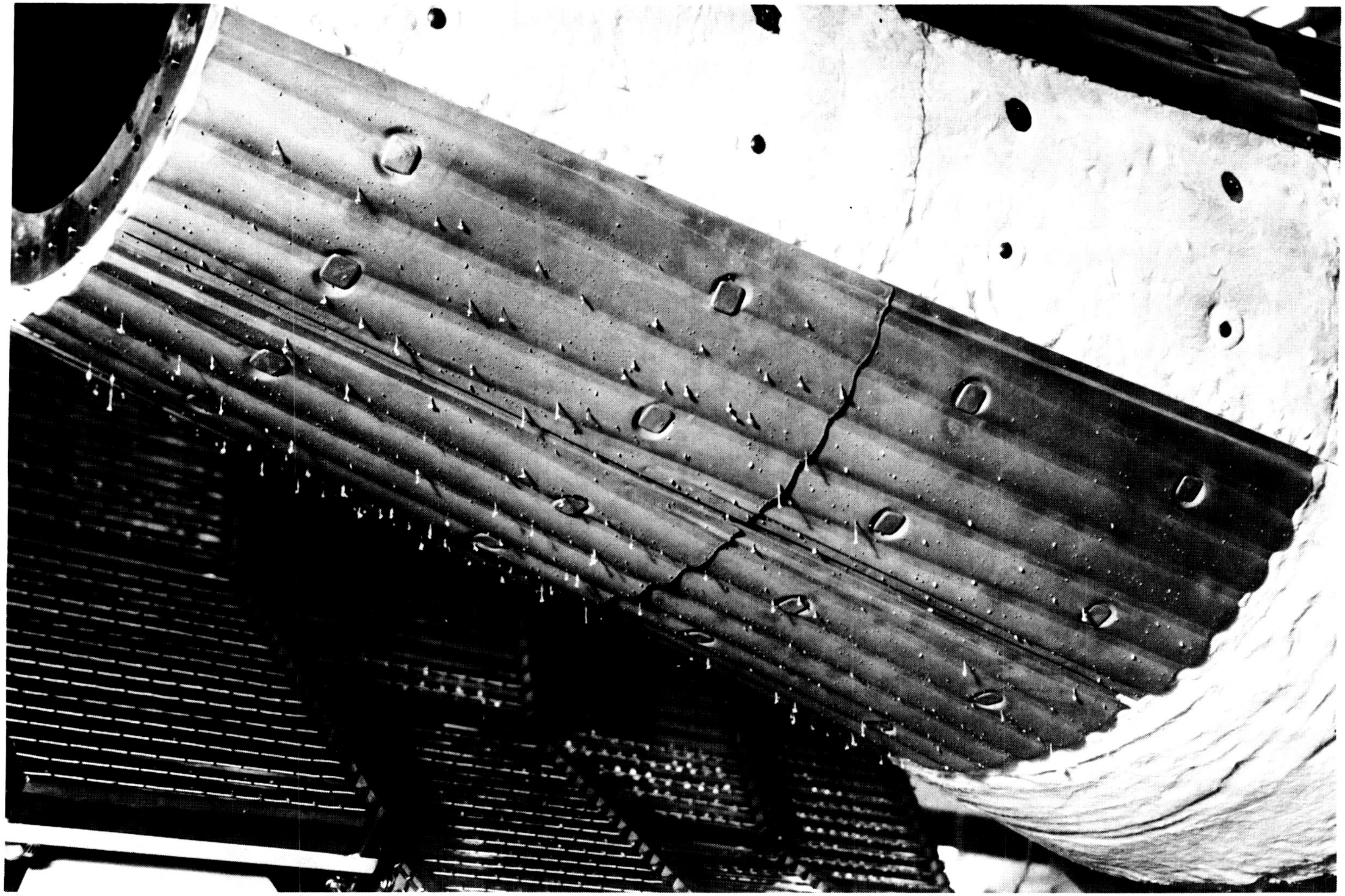

Figure 30.- Coated tantalum-alloy shields after initial aborted cycle to a maximum temperature of 2100° F (1420 K). L-68-9724

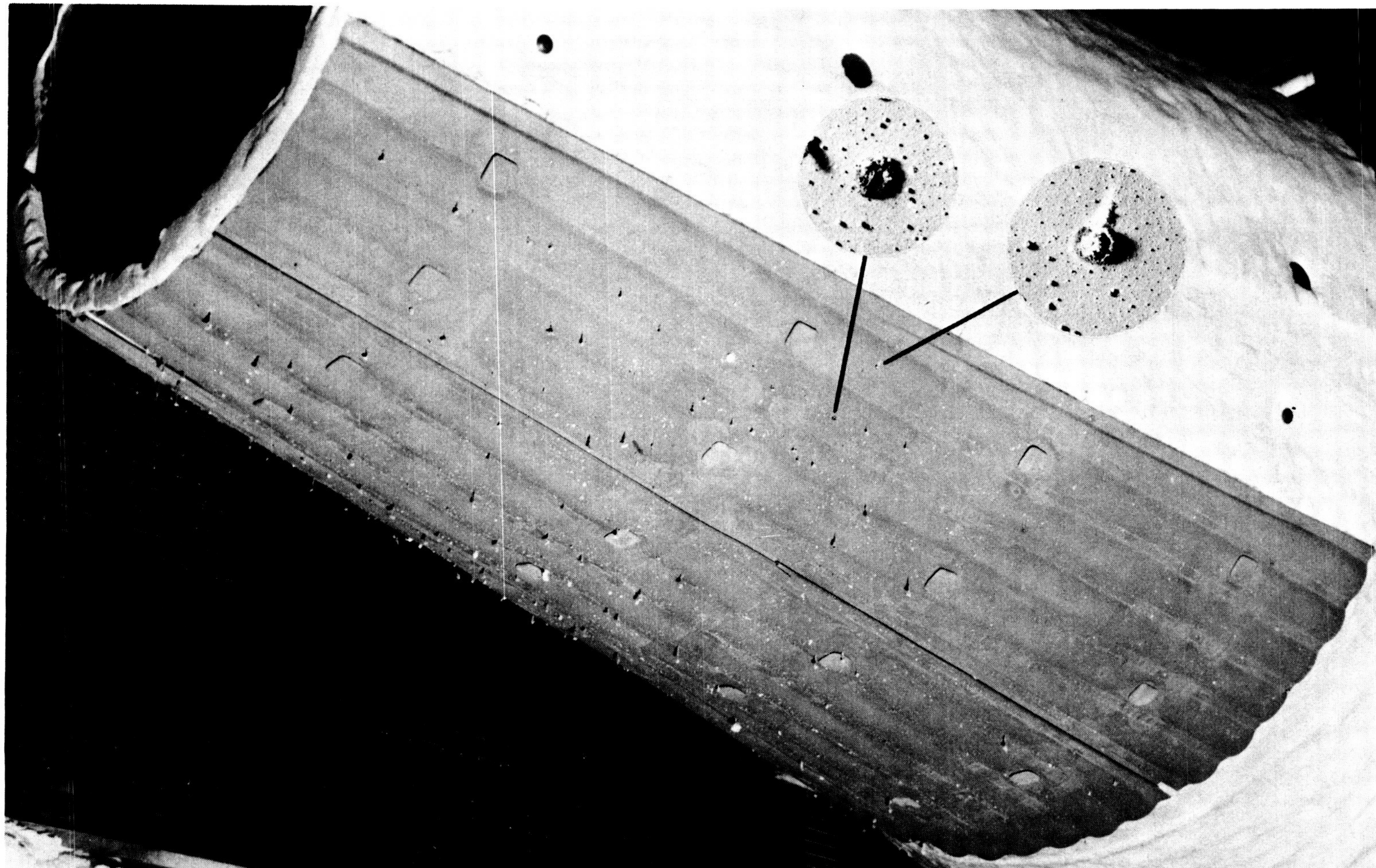

Figure 31.- Coated tantalum-alloy shields after first 2600° F (1700 K) profile with enlargements of oxidation failures. L-68-9762.1

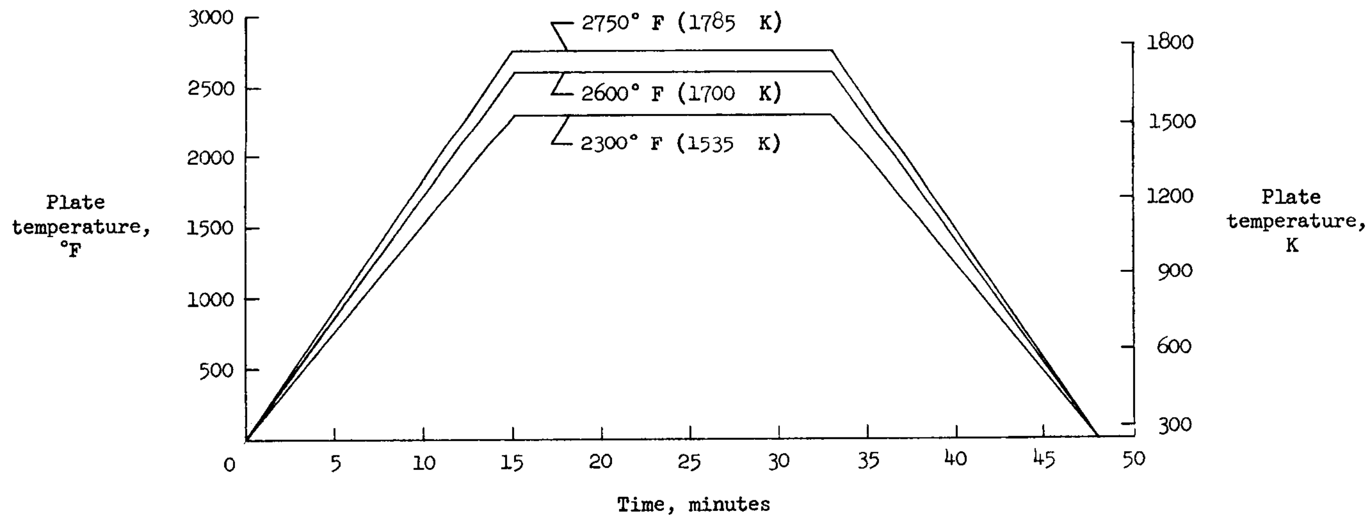

(a) Temperature profiles for probe calibration.

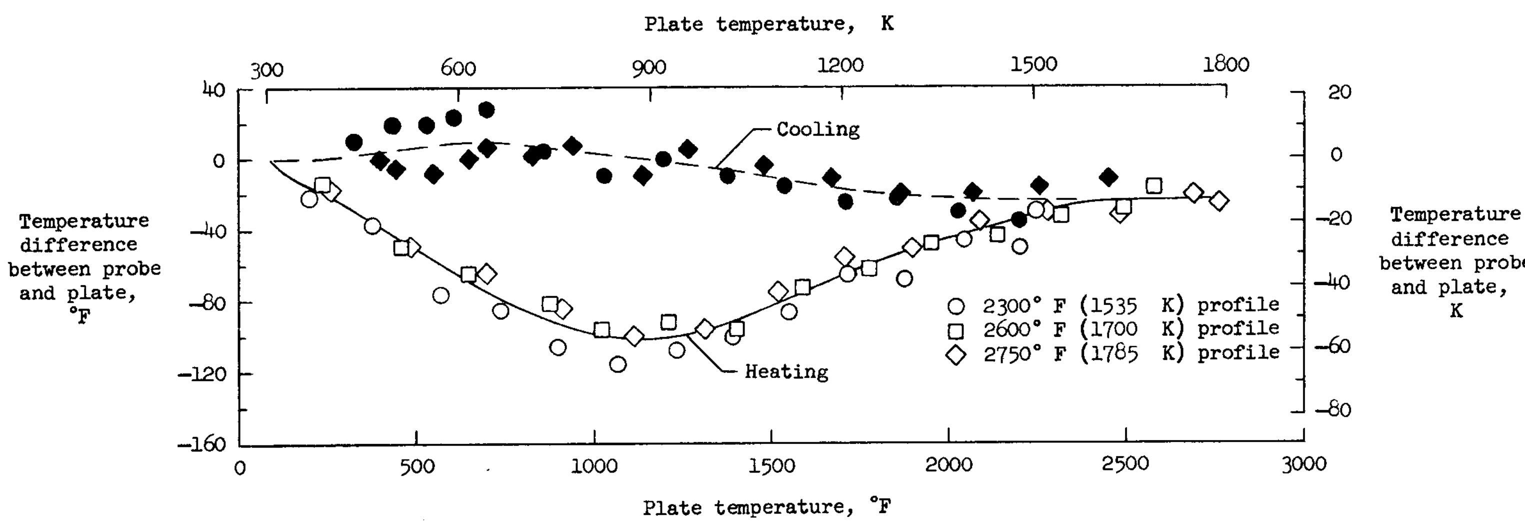

(b) Probe temperature response compared with plate temperature response.

Figure 32.- Results of thermocouple calibration tests to determine temperature response of thermocouple probe compared with spotwelded thermocouple.